Relativistic effects in Physics and Astrophysics

Contents

1. Topics

- The Gamma-Ray Burst (GRB) luminosity evolution over the equitemporal surfaces (EQTS).

- The apparent radius of the equitemporal surfaces in the sky.

- Exact versus approximate equations of motion.

- Exact analytic expressions for the EQTS.

- Exact versus approximate beaming formulas.

- Interaction of the ultrarelativistically expanding plasma, emitting the GRB, with the remnants of the progenitor binary system.

2. Participants

2.1. ICRANet participants

- Carlo Luciano Bianco

- Remo Ruffini

- Gregory Vereshchagin

- She-Sheng Xue

2.2. Past collaborators

- Christian Cherubini (Università "Campus Biomedico", Italy)

- Jurgen Ehlers (Max-Plank Institut, Germany)

- Federico Fraschetti (CEA Saclay, France)

- Eliana La Francesca (Undergraduate, Italy)

- Francesco Alessandro Massucci (Undergraduate, Italy)

2.3. Students

- David Melon Fuksman (IRAP PhD, Italy)

3. Brief description

3.1. Highlights of recent results

3.1.1. The luminosity evolution over the equitemporal surfaces in the prompt emission of Gamma-Ray Bursts

It is widely accepted that Gamma-Ray Burst (GRB) afterglows originate from the interaction of an ultrarelativistically expanding shell into the CircumBurst Medium (CBM). Differences exists on the detailed kinematics and dynamics of such a shell (see e.g. Bianco and Ruffini, 2005a; Meszaros, 2006, and refs. therein).

Due to the ultrarelativistic velocity of the expanding shell (Lorentz gamma factor $\gamma \sim 10^2 - 10^3$), photons emitted at the same time in the laboratory frame (i.e. the one in which the center of the expanding shell is at rest) from the shell surface but at different angles from the line of sight do not reach the observer at the same arrival time. Therefore, if we were able to resolve spatially the GRB afterglows, we would not see the spherical surface of the shell. We would see instead the projection on the celestial sphere of the EQuiTemporal Surface (EQTS), defined as the surface locus of points which are source of radiation reaching the observer at the same arrival time (see e.g. Couderc, 1939; Rees, 1966; Sari, 1998; Panaitescu and Meszaros, 1998; Granot et al., 1999a; Bianco et al., 2001; Bianco and Ruffini, 2004, 2005b, and refs. therein). The knowledge of the exact shape of the EQTSs is crucial, since any theoretical model must perform an integration over the EQTSs to compute any prediction for the observed quantities (see e.g. Gruzinov and Waxman, 1999; Oren et al., 2004; Bianco and Ruffini, 2004, 2005b; Granot et al., 2005; Meszaros, 2006; Huang et al., 2006, 2007, and refs. therein).

One of the key problems is the determination of the angular size of the visible region of each EQTS, as well as the distribution of the luminosity over such a visible region. In the current literature it has been shown that in the latest afterglow phases the luminosity is maximum at the boundaries of the visible region and that the EQTS must then appear as expanding luminous "rings" (see e.g. Waxman, 1997; Sari, 1998; Panaitescu and Meszaros, 1998; Granot et al., 1999a,b; Waxman et al., 1998; Galama et al., 2003; Granot and Loeb, 2003; Taylor et al., 2004; Granot, 2008, and refs. therein). Such an anal-

ysis is applied only in the latest afterglow phases to interpret data from radio observations (Frail et al., 1997; Waxman et al., 1998; Galama et al., 2003; Taylor et al., 2004; Granot et al., 2005; Taylor et al., 2005; Pihlström et al., 2007) or gravitational microlensing (Garnavich et al., 2000; Gaudi et al., 2001; Ioka and Nakamura, 2001; Granot and Loeb, 2001). The shell dynamics is usually assumed to be fully adiabatic and to be described by a power-law $\gamma \propto r^{-3/2}$, following the Blandford and McKee (1976) self similar solution, where γ and r are respectively the Lorentz gamma factor and the radius of the expanding shell. Such a power-law behavior has been extrapolated backward from the latest phases of the afterglow all the way to the prompt emission phase.

In Bianco and Ruffini (2004, 2005b,a) there have been presented the analytic solutions of the equations of motion for GRB afterglow, compared with such approximate solutions, both in the fully radiative and adiabatic regimes, and the corresponding analytic expressions for the EQTSs. It has been shown that the approximate power-law regime can be asymptotically reached by the Lorentz gamma factor only in the latest afterglow phases, when $\gamma \sim 10$, and only if the initial Lorentz gamma factor $\gamma_\circ$ of the shell satisfies $\gamma_\circ > 10^2$ in the adiabatic case or $\gamma_\circ > 10^4$ in the radiative case. Therefore, in no way the approximate power-law solution can be used to describe the previous dynamical phases of the shell, which are the relevant ones for the prompt emission and for the early afterglow.

Starting from these premises, in the appendix "The luminosity evolution over the EQuiTemporal Surfaces in the prompt emission of Gamma-Ray Bursts" (see section A) we present the distribution of the extended afterglow luminosity over the visible region of a single EQTSs within the "fireshell" model for GRBs. Such a model uses the exact solutions of the fireshell equations of motion and assumes a fully radiative dynamics (see Ruffini et al., 2001a, 2009, and refs. therein for details). We recall that within the fireshell model the peak of the extended afterglow encompasses the prompt emission. We focus our analysis on the prompt emission and the early afterglow phases. Our approach is therefore complementary to the other ones in the current literature, which analyze only the latest afterglow phases, and it clearly leads to new results when applied to the prompt emission phase. For simplicity, we consider only the bolometric luminosity (Ruffini et al., 2002), since during the prompt phase this is a good approximation of the one observed e.g. by BAT or GBM instruments (Ruffini et al., 2002, 2004b). The analysis is separately performed over different selected EQTSs. The temporal evolution of the luminosity distribution over the EQTSs' visible region is presented. As a consequence of these results, we show the novel feature that at the beginning of the prompt emission the most luminous regions of the EQTSs are the ones closest to the line of sight. On the contrary, in the late prompt emission and in the early afterglow phases the most luminous EQTS regions are the ones

closest to the boundary of the visible region.

3.1.2. The apparent size of equitemporal surfaces in the sky

A consequence of the results presented above is that we were able to derive an analytic expression for the temporal evolution, measured in arrival time, of the apparent size of the EQTSs in the sky, valid in both the fully radiative and the adiabatic regimes. Such an expression is presented in the appendix "The apparent radius of the equitemporal surfaces in the sky" (section B). We will also discuss analogies and differences with other approaches in the current literature which assumes an adiabatic dynamics instead of a fully radiative one.

3.2. Appendix on previous results

3.2.1. Exact versus approximate solutions in Gamma-Ray Burst afterglows

In the appendix "Exact versus approximate solutions in Gamma-Ray Burst afterglows" (section C) we first write the energy and momentum conservation equations for the interaction between the ABM pulse and the Circum-Burst Medium (CBM) in a finite difference formalism, already discussed in the previous report about "Gamma-Ray Bursts". We then express these same equations in a differential formalism to compare our approach with the ones in the current literature. We write the exact analytic solutions of such differential equations both in the fully radiative and in the adiabatic regimes. We then compare and contrast these results with the ones following from the ultra-relativistic approximation widely adopted in the current literature. Such an ultra-relativistic approximation, adopted to apply to Gamma-Ray Bursts (GRBs) the Blandford and McKee (1976) self-similar solution, led to a simple power-law dependence of the Lorentz gamma factor of the baryonic shell on the distance. On the contrary, we show that no constant-index power-law relations between the Lorentz gamma factor and the distance can exist, both in the fully radiative and in the adiabatic regimes. The exact solution is indeed necessary if one wishes to describe properly all the phases of the afterglow including the prompt emission.

3.2.2. Exact analytic expressions for the equitemporal surfaces in Gamma-Ray Burst afterglows

In the appendix "Exact analytic expressions for the equitemporal surfaces in Gamma-Ray Burst afterglows" (section D) we follow the indication by Paul Couderc (1939) who pointed out long ago how in all relativistic expansions the crucial geometrical quantities with respect to a physical observer are the "equitemporal surfaces" (EQTSs), namely the locus of source points of the signals arriving at the observer at the same time. After recalling the formal definition of the EQTSs, we use the exact analytic solutions of the equations of motion recalled in the previous section to derive the exact analytic expressions of the EQTSs in GRB afterglow both in the fully radiative and adiabatic regimes. We then compare and contrast such exact analytic solutions with the corresponding ones widely adopted in the current literature and computed using the approximate "ultra-relativistic" equations of motion discussed in the previous section. We show that the approximate EQTS expressions lead to uncorrect estimates of the size of the ABM pulse when compared to the exact ones. Quite apart from their academic interest, these results are crucial for the interpretation of GRB observations: all the observables come in fact from integrated quantities over the EQTSs, and any minor disagreement in their definition can have extremely drastic consequences on the identification of the true physical processes.

3.2.3. Exact versus approximate beaming formulas in Gamma-Ray Burst afterglows

In the appendix "Exact versus approximate beaming formulas in Gamma-Ray Burst afterglows" (section E) we discuss the possibility that GRBs originate from a beamed emission, one of the most debated issue about the nature of the GRB sources in the current literature after the work by Mao and Yi (1994) (see e.g. Piran, 2005; Meszaros, 2006, and references therein). In particular, on the ground of the theoretical considerations by Sari et al. (1999), it was conjectured that, within the framework of a conical jet model, one may find that the gamma-ray energy released in all GRBs is narrowly clustered around 5×10^{50} ergs (Frail et al., 2001). We have never found in our GRB model any necessity to introduce a beamed emission. Nevertheless, we have considered helpful and appropriate helping the ongoing research by giving the exact analytic expressions of the relations between the detector arrival time t_a^d of the GRB afterglow radiation and the corresponding half-opening angle ϑ of the expanding source visible area due to the relativistic beaming. We have done this both in the fully radiative and in the adiabatic regimes, us-

ing the exact analytic solutions presented in the previous sections. Again, we have compared and contrasted our exact solutions with the approximate ones widely used in the current literature. We have found significant differences, particularly in the fully radiative regime which we consider the relevant one for GRBs, and it goes without saying that any statement on the existence of beaming can only be considered meaningful if using the correct equations.

4. Publications on refereed journals

1. C.L. Bianco, R. Ruffini; "Exact versus approximate equitemporal surfaces in Gamma-Ray Burst afterglows"; The Astrophysical Journal, 605, L1 (2004).

   By integrating the relativistic hydrodynamic equations introduced by Taub we have determined the exact EQuiTemporal Surfaces (EQTSs) for the Gamma-Ray Burst (GRB) afterglows. These surfaces are compared and contrasted to the ones obtained, using approximate methods, by Panaitescu and Meszaros (1998); Sari (1998); Granot et al. (1999a).

2. C.L. Bianco, R. Ruffini; "On the exact analytic expressions for the equitemporal surfaces in Gamma-Ray Burst afterglows"; The Astrophysical Journal, 620, L23 (2005).

   We have recently shown (see Bianco and Ruffini, 2004) that marked differences exist between the EQuiTemporal Surfaces (EQTSs) for the Gamma-Ray Burst (GRB) afterglows numerically computed by the full integration of the equations of motion and the ones found in the current literature expressed analytically on the grounds of various approximations. In this Letter the exact analytic expressions of the EQTSs are presented both in the case of fully radiative and adiabatic regimes. The new EQTS analytic solutions validate the numerical results obtained in Bianco and Ruffini (2004) and offer a powerful tool to analytically perform the estimates of the physical observables in GRB afterglows.

3. C.L. Bianco, R. Ruffini; "Exact versus approximate solutions in Gamma-Ray Burst afterglows"; The Astrophysical Journal, 633, L13 (2005).

   We have recently obtained the exact analytic solutions of the relativistic equations relating the radial and time coordinate of a relativistic thin uniform shell expanding in the interstellar medium in the fully radiative and fully adiabatic regimes. We here re-examine the validity of the constant-index power-law relations between the Lorentz gamma factor and its radial coordinate, usually adopted in the current Gamma-Ray Burst (GRB) literature on the grounds of an "ultrarelativistic" approximation. Such expressions are found to be mathematically correct but only approximately valid in a very limited range of the physical and astrophysical parameters and in an asymptotic regime which is

reached only for a very short time, if any, and are shown to be not applicable to GRBs.

4. C.L. Bianco, R. Ruffini; "Exact versus approximate beaming formulae in Gamma-Ray Burst afterglows"; The Astrophysical Journal, 644, L105 (2006).

We present the exact analytic expressions to compute, assuming the emitted Gamma-Ray Burst (GRB) radiation is not spherically symmetric but is confined into a narrow jet, the value of the detector arrival time at which we start to "see" the sides of the jet, both in the fully radiative and adiabatic regimes. We obtain this result using our exact analytic expressions for the EQuiTemporal Surfaces (EQTSs) in GRB afterglows. We re-examine the validity of three different approximate formulas currently adopted for the adiabatic regime in the GRB literature. We also present an empirical fit of the numerical solutions of the exact equations, compared and contrasted with the three above approximate formulas. The extent of the differences is such as to require a reassessment on the existence and entity of beaming in the cases considered in the current literature, as well as on its consequences on the GRB energetics.

5. C.L. Bianco, F.A. Massucci, R. Ruffini: "The luminosity evolution over the EQuiTemporal Surfaces in the prompt emission of Gamma-Ray Bursts"; Int. J. Mod. Phys D, 20, 1919 (2011).

Due to the ultrarelativistic velocity of the expanding "fireshell" (Lorentz gamma factor $\gamma \sim 10^2 - 10^3$), photons emitted at the same time from the fireshell surface do not reach the observer at the same arrival time. In interpreting Gamma-Ray Bursts (GRBs) it is crucial to determine the properties of the EQuiTemporal Surfaces (EQTSs): the locus of points which are source of radiation reaching the observer at the same arrival time. In the current literature this analysis is performed only in the latest phases of the afterglow. Here we study the distribution of the GRB bolometric luminosity over the EQTSs, with special attention to the prompt emission phase. We analyze as well the temporal evolution of the EQTS apparent size in the sky. We use the analytic solutions of the equations of motion of the fireshell and the corresponding analytic expressions of the EQTSs which have been presented in recent works and which are valid for both the fully radiative and the adiabatic dynamics. We find the novel result that at the beginning of the prompt emission the most luminous regions of the EQTSs are the ones closest to the line of sight. On the contrary, in the late prompt emission and in the early afterglow phases the most luminous EQTS regions are the ones closest to the boundary of the visible region. This transition in the emitting region may lead to specific observational signatures, i.e. an anomalous spectral evolution, in the rising part or at the peak

of the prompt emission. We find as well an expression for the apparent radius of the EQTS in the sky, valid in both the fully radiative and the adiabatic regimes. Such considerations are essential for the theoretical interpretation of the prompt emission phase of GRBs.

A. The luminosity evolution over the EQuiTemporal Surfaces in the prompt emission of Gamma-Ray Bursts

A.1. The Equitemporal surfaces (EQTS)

For the case of a spherically symmetric fireshell considered in this Letter, the EQTSs are surfaces of revolution about the line of sight. The general expression for their profile, in the form $\vartheta = \vartheta(r)$, corresponding to an arrival time t_a of the photons at the detector, can be obtained from (e.g. Bianco and Ruffini, 2005b):

$$ct_a = ct\,(r) - r\cos\vartheta + r^\star\,, \qquad (A.1.1)$$

where $r^\star$ is the initial size of the expanding fireshell, ϑ is the angle between the radial expansion velocity of a point on its surface and the line of sight, $t = t(r)$ is its equation of motion, expressed in the laboratory frame, and c is the speed of light.

In the case of a fully radiative regime, the dynamics of the system is given by the following solution of the equations of motion (e.g. Piran, 1999; Bianco and Ruffini, 2005b, and refs. therein):

$$\gamma = \frac{1 + (M_{\mathrm{cbm}}/M_B)\left(1 + \gamma_\circ^{-1}\right)\left[1 + (1/2)\left(M_{\mathrm{cbm}}/M_B\right)\right]}{\gamma_\circ^{-1} + (M_{\mathrm{cbm}}/M_B)\left(1 + \gamma_\circ^{-1}\right)\left[1 + (1/2)\left(M_{\mathrm{cbm}}/M_B\right)\right]}\,, \qquad (A.1.2)$$

where γ is the Lorentz gamma factor of the fireshell, M_{cbm} is the amount of CBM mass swept up within the radius r and $\gamma_\circ$ and M_B are respectively the values of the Lorentz gamma factor and of the mass of the fireshell at the beginning of the extended afterglow phase. Correspondingly, the exact

analytic expression for $t = t(r)$ is (Bianco and Ruffini, 2005b):

$$t\left(r\right) = \frac{(M_B - m_i^\circ)(r - r_\circ)}{2c\sqrt{C}} + \frac{r_\circ\sqrt{3C}}{6cm_i^\circ A^2}\left[\arctan\frac{2r - Ar_\circ}{Ar_\circ\sqrt{3}} - \arctan\frac{2 - A}{A\sqrt{3}}\right]$$

$$+ \frac{r_\circ\sqrt{C}}{12cm_i^\circ A^2}\ln\left\{\frac{[A + (r/r_\circ)]^3(A^3 + 1)}{[A^3 + (r/r_\circ)^3](A+1)^3}\right\} + t_\circ + \frac{m_i^\circ r_\circ}{8c\sqrt{C}}\left(\frac{r^4 - r_\circ^4}{r_\circ^4}\right), \qquad \text{(A.1.3)}$$

where $A = \sqrt[3]{(M_B - m_i^\circ)/m_i^\circ}$, $C = M_B{}^2(\gamma_\circ - 1)/(\gamma_\circ + 1)$, $t_\circ$ is the value of the time t at the beginning of the extended afterglow phase and $m_i^\circ = (4/3)\pi m_p n_{\text{cbm}} r_\circ^3$. Inserting Eq.(A.1.3) into Eq.(A.1.1) we have the analytic expression for the EQTS in the fully radiative regime (Bianco and Ruffini, 2005b):

$$\cos\vartheta = \frac{(M_B - m_i^\circ)(r - r_\circ)}{2r\sqrt{C}} + \frac{r_\circ\sqrt{3C}}{6rm_i^\circ A^2}\left[\arctan\frac{2r - Ar_\circ}{Ar_\circ\sqrt{3}} - \arctan\frac{2 - A}{A\sqrt{3}}\right]$$

$$+ \frac{m_i^\circ r_\circ}{8r\sqrt{C}}\left(\frac{r^4 - r_\circ^4}{r_\circ^4}\right) + \frac{r_\circ\sqrt{C}}{12rm_i^\circ A^2}\ln\left\{\frac{[A + (r/r_\circ)]^3(A^3 + 1)}{[A^3 + (r/r_\circ)^3](A+1)^3}\right\} + \frac{ct_\circ - ct_a + r^\star}{r}. \qquad \text{(A.1.4)}$$

Instead, the corresponding equations in the adiabatic regime are (Bianco and Ruffini, 2005b):

$$\gamma^2 = \frac{\gamma_\circ^2 + 2\gamma_\circ\left(M_{\text{cbm}}/M_B\right) + \left(M_{\text{cbm}}/M_B\right)^2}{1 + 2\gamma_\circ\left(M_{\text{cbm}}/M_B\right) + \left(M_{\text{cbm}}/M_B\right)^2}, \qquad \text{(A.1.5)}$$

$$t\left(r\right) = \left(\gamma_\circ - \frac{m_i^\circ}{M_B}\right)\frac{r - r_\circ}{c\sqrt{\gamma_\circ^2 - 1}} + \frac{m_i^\circ}{4M_B r_\circ^3}\left(\frac{r^4 - r_\circ^4}{c\sqrt{\gamma_\circ^2 - 1}}\right) + t_\circ, \qquad \text{(A.1.6)}$$

$$\cos\vartheta = \frac{m_i^\circ}{4M_B\sqrt{\gamma_\circ^2 - 1}}\left(\frac{r^4 - r_\circ^4}{r_\circ^3 r}\right) + \frac{ct_\circ - ct_a + r^\star}{r} - \frac{\gamma_\circ - \left(m_i^\circ/M_B\right)}{\sqrt{\gamma_\circ^2 - 1}}\left(\frac{r_\circ - r}{r}\right). \qquad \text{(A.1.7)}$$

A comparison between the Lorentz gamma factors in the two regimes is presented in Fig. A.1. Here and in the following we assume the same initial conditions as in Bianco and Ruffini (2005b), namely $\gamma_\circ = 310.131$, $r_\circ = 1.943 \times 10^{14}$ cm, $t_\circ = 6.481 \times 10^3$ s, $r^\star = 2.354 \times 10^8$ cm, $n_{cbm} = 1.0\,\text{particles}/\text{cm}^3$, $M_B = 1.61 \times 10^{30}$ g. For simplicity, and since we are interested in the overall behavior of the luminosity distribution, we assume a constant CBM density, neglecting the inhomogeneities which are responsible of the temporal variability of the prompt emission (Ruffini et al., 2002).
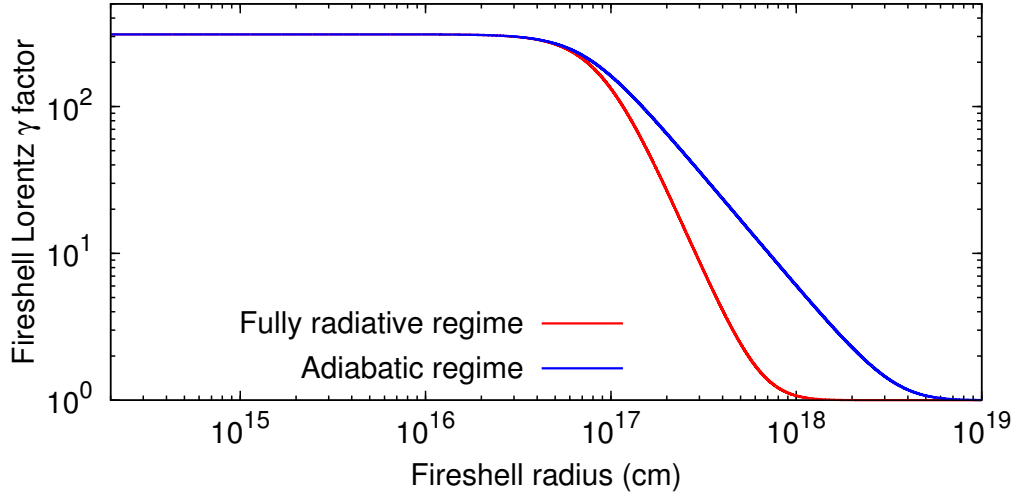
Figure A.1.: The Fireshell Lorentz gamma factors in the fully radiative regime (red line), given by Eq.(A.1.2), and in the adiabatic regime (blue line), given by Eq.(A.1.5).

A.2. The extended afterglow luminosity distribution over the EQTS

Within the fireshell model, the GRB extended afterglow bolometric luminosity in an arrival time dt_a and per unit solid angle $d\Omega$ is given by (details in Ruffini et al., 2009, and refs. therein):

$$\frac{dE_\gamma}{dt_a d\Omega} \equiv \int_{EQTS} \mathcal{L}(r, \vartheta, \varphi; t_a) d\Sigma = \int_{EQTS} \frac{\Delta\varepsilon \cos\vartheta v dt}{4\pi\Lambda^4 dt_a} d\Sigma, \qquad (A.2.1)$$

where $\Delta\varepsilon$ is the energy density released in the interaction of the ABM pulse with the CBM measured in the comoving frame, $\Lambda = \gamma(1 - (v/c)\cos\vartheta)$ is the Doppler factor, $d\Sigma$ is the surface element of the EQTS at arrival time t_a on which the integration is performed, and it has been assumed the fully radiative condition. We are here not considering the cosmological redshift of the source, which is constant during the GRB explosion and therefore it cannot affect the results of the present analysis. We recall that in our case such a bolometric luminosity is a good approximation of the one observed in the prompt emission and in the early afterglow by e.g. the BAT or GBM instruments (Ruffini et al., 2002, 2004b).

We are now going to show how this luminosity is distributed over the EQTSs, i.e. we are going to plot over selected EQTSs the luminosity density $\mathcal{L}(r, \vartheta, \varphi; t_a)$. The results are represented in Fig. A.2. We chose eight differ-
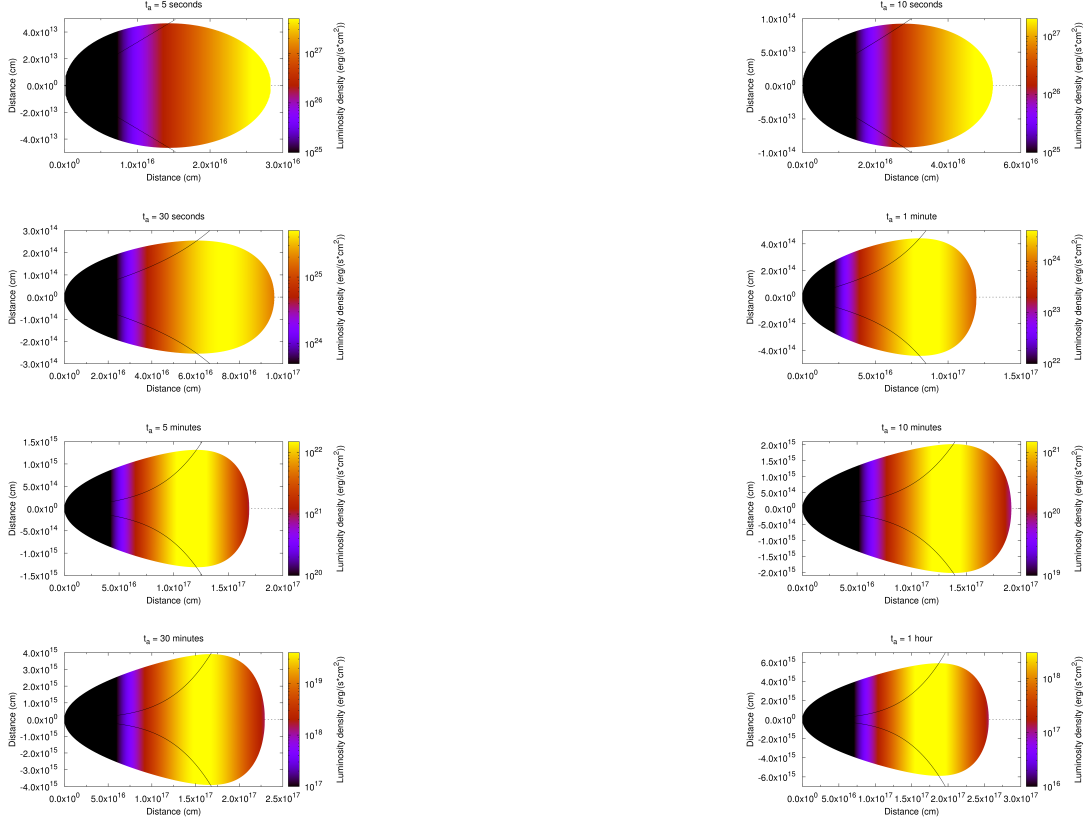
Figure A.2.: We plot the luminosity density $\mathcal{L}$ given in Eq.(A.2.1) over 8 different EQTSs, corresponding to 8 different t_a values ranging from the prompt emission (5 seconds) to the early (1 hour) afterglow phases (see title above each plot). Each EQTS is represented as its projection on a plane containing the line of sight, which coincides with the X axis of each plot and which is represented by a dashed gray line. The observer is far away along the X axis. The luminosity density distribution over each EQTS is represented by a color gradient, with the highest values corresponding to the lightest colors (see the key on the left of each plot). The scales of the different axes and of the color gradient are different among the different plots, since it was not possible to choose a single scale suitable for all of them. The black curves represent the condition $\cos\vartheta = v/c$, see Eq.(A.2.2). The boundaries of the visible regions are therefore defined by the intersections of such lines with the EQTS external profiles, which coincide with the points where the EQTS external profiles show an horizontal tangent in the plots.

ent EQTSs, corresponding to arrival time values ranging from the prompt emission (5 seconds) to the early (1 hour) afterglow phases. For each EQTS we represent also the boundaries of the visible region due to relativistic collimation, defined by the condition (see e.g. Bianco and Ruffini, 2006, and refs. therein):

$$\cos\vartheta \geq v/c. \tag{A.2.2}$$

We obtain that, at the beginning ($t_a = 5$ seconds), when γ is approximately constant, the most luminous regions of the EQTS are the ones along the line of sight. However, as γ starts to drop ($t_a \gtrsim 30$ seconds), the most luminous regions of the EQTSs become the ones closest to the boundary of the visible region. This transition in the emitting region may lead to specific observational signatures, i.e. an anomalous spectral evolution, in the rising part or at the peak of the prompt emission.

A.3. Conclusions

Within the fireshell model, using the exact analytic expressions for the fireshell equations of motion and for the corresponding EQTSs in the fully radiative condition, we analyzed the temporal evolution of the distribution of the extended afterglow luminosity over the EQTS during the prompt emission and the early afterglow phases. We find that, at the beginning of the prompt emission ($t_a = 5$ seconds), when γ is approximately constant, the most luminous regions of the EQTS are the ones along the line of sight. As γ starts to drop ($t_a \gtrsim 30$ seconds), the most luminous regions of the EQTSs become the ones closest to the boundary of the visible region. This transition in the emitting region may lead to specific observational signatures, i.e. an anomalous spectral evolution, in the rising part or at the peak of the prompt emission. The EQTSs of GRB extended afterglows should therefore appear in the sky as point-like sources at the beginning of the prompt emission but evolving after a few seconds into expanding luminous "rings", with an apparent radius evolving in time and always equal to the maximum transverse EQTS visible radius $r_\perp$.

B. The apparent radius of the equitemporal surfaces in the sky

From sec. A.2 we obtain that within the fireshell model the EQTSs of GRB extended afterglows should appear in the sky as point-like sources at the beginning of the prompt emission but evolving after a few seconds into expanding luminous "rings", with an apparent radius evolving in time and always equal to the maximum transverse EQTS visible radius $r_\perp$ which can be obtained from Eqs.(A.1.1,A.2.2):

$$\begin{cases} r_\perp = r \sin \vartheta \\ ct_a = ct\,(r) - r \cos \vartheta + r^\star \\ \cos \vartheta = v/c \end{cases} . \tag{B.0.1}$$

where $t = t(r)$ is given by Eq.(A.1.3). With a small algebra we get:

$$\begin{cases} r_\perp = r/\gamma(r) \\ t_a = t(r) - (r/c)\sqrt{1 - \gamma(r)^{-2}} + (r^\star/c) \end{cases} , \tag{B.0.2}$$

where $\gamma \equiv \gamma\,(r)$ is given by Eq.(A.1.2) and $t \equiv t\,(r)$ is given by Eq.(A.1.3), since we assumed the fully radiative condition. Eq.(B.0.2) defines parametrically the evolution of $r_\perp \equiv r_\perp\,(t_a)$, i.e. the evolution of the maximum transverse EQTS visible radius as a function of the arrival time. In Fig. A.2 we saw that such $r_\perp$ coincides with the actual value of the EQTS apparent radius in the sky only for $t_a \gtrsim 30$ s, since for $t_a \lesssim 30$ s the most luminous EQTS regions are the ones closest to the line of sight (see the first three plots in Fig. A.2). Therefore, in Fig. B.1 we plot $r_\perp$ given by Eq.(B.0.2) in the fully radiative regime together with the actual values of the EQTS apparent radius in the sky taken from Fig. A.2 in the three cases in which they are different. It is clear that, during the early phases of the prompt emission, even the "exact solution" given by Eq.(B.0.2) can be considered only an upper limit to the actual EQTS apparent radius in the sky.

In the current literature (see e.g. Sari, 1998; Waxman et al., 1998; Granot et al., 1999a,b; Garnavich et al., 2000; Granot and Loeb, 2001; Gaudi et al., 2001; Galama et al., 2003; Granot and Loeb, 2003; Taylor et al., 2004; Oren et al., 2004; Granot et al., 2005; Granot, 2008) there are no analogous treat-

Figure B.1.: The EQTS apparent radius in the sky as a function of the arrival time t_a in the fully radiative regime. The red line represents the maximum transverse EQTS visible radius $r_\perp$ following Eq.(B.0.2). The three blue points represents the actual EQTS apparent radius in the sky in the three cases $t_a = 5.0$ s, $t_a = 10.0$ s and $t_a = 30.0$ s in which, as shown in Fig. A.2, it is smaller than $r_\perp$. The blue line is a linear interpolation of such points.

ments, since it is always assumed an adiabatic dynamics instead of a fully radiative one and only the latest afterglow phases are addressed. It is usually assumed the Blandford and McKee (1976) self similar solution for the adiabatic dynamics $\gamma \propto r^{-3/2}$. A critical analysis of the applicability to GRBs of this approximate dynamics, instead of the exact solutions in Eqs.(A.1.5,A.1.6,A.1.7), has been presented in Bianco and Ruffini (2005a), as recalled in the introduction. The most widely applied formula for the EQTS apparent radius in the above mentioned current literature is the one proposed by Sari (1998):

$$r_\perp = 3.91 \times 10^{16} \left(E_{52}/n_1 \right)^{1/8} \left[T_{days}/(1+z) \right]^{5/8} \text{ cm,} \qquad \text{(B.0.3)}$$

where E_{52} is the initial energy of the shell in units of 10^{52} ergs, n_1 is the CBM density in units of 1 particle/cm^3, T_{days} is the arrival time at the detector of the radiation measured in days, and z is the source cosmological redshift. Waxman et al. (1998) however derived a numerical factor of 3.66×10^{16} instead of 3.91×10^{16}. Eq.(B.0.3) cannot be compared directly with Eq.(B.0.2), since they assume two different dynamical regimes. Therefore, we first plot in Fig. B.2 the exact solution for $r_\perp$ given by Eq.(B.0.2) both in the fully radiative case, using Eqs.(A.1.2,A.1.3), and in the adiabatic one, using Eqs.(A.1.5,A.1.6). We see that they almost coincide during the prompt emission while they start to diverge in the early afterglow phases, following the behavior of the corresponding Lorentz gamma factors (see Fig. A.1 and details in Bianco and Ruffini, 2005a).

Now, in Fig. B.3 and for the same initial conditions assumed in previous figures, we plot the maximum transverse EQTS visible radius $r_\perp$ given by Eq.(B.0.2) in the adiabatic case, using Eqs.(A.1.5,A.1.6), together with Eq.(B.0.3), proposed by Sari (1998), and with the corresponding modification in the numerical factor proposed by Waxman et al. (1998). From such a comparison, we can see that the approximate regime $r_\perp \propto t_a^{5/8}$ overestimates the exact solution for $r_\perp$ during the prompt emission and the early afterglow phases. It is asymptotically reached only in the latest afterglow phases ($t_a \gtrsim 10^3$ s), in the very small region in which the approximate power-law dynamics starts to be applicable (see details in Bianco and Ruffini, 2005a). However, there is still a small discrepancy in the normalization: the constant numerical factor in front of Eq.(B.0.3) should be $\sim 3.1 \times 10^{16}$ instead of 3.91×10^{16} or 3.66×10^{16} to reproduce the behavior of the exact solution for large t_a. Moreover, we must emphasize that, in analogy with what we obtained in the fully radiative case (see Fig. B.1), in the early phases of the prompt emission, when the fireshell Lorentz γ factor is almost constant, the maximum transverse EQTS visible radius $r_\perp$ given by Eq.(B.0.2) can only be considered an upper limit to the actual value of the EQTS apparent radius in the sky. In such phases the

Figure B.2.: Comparison between the maximum transverse EQTS visible radius $r_\perp$ computed with Eq.(B.0.2) in the adiabatic (blue line) and in the fully radiative (red line) cases respectively.
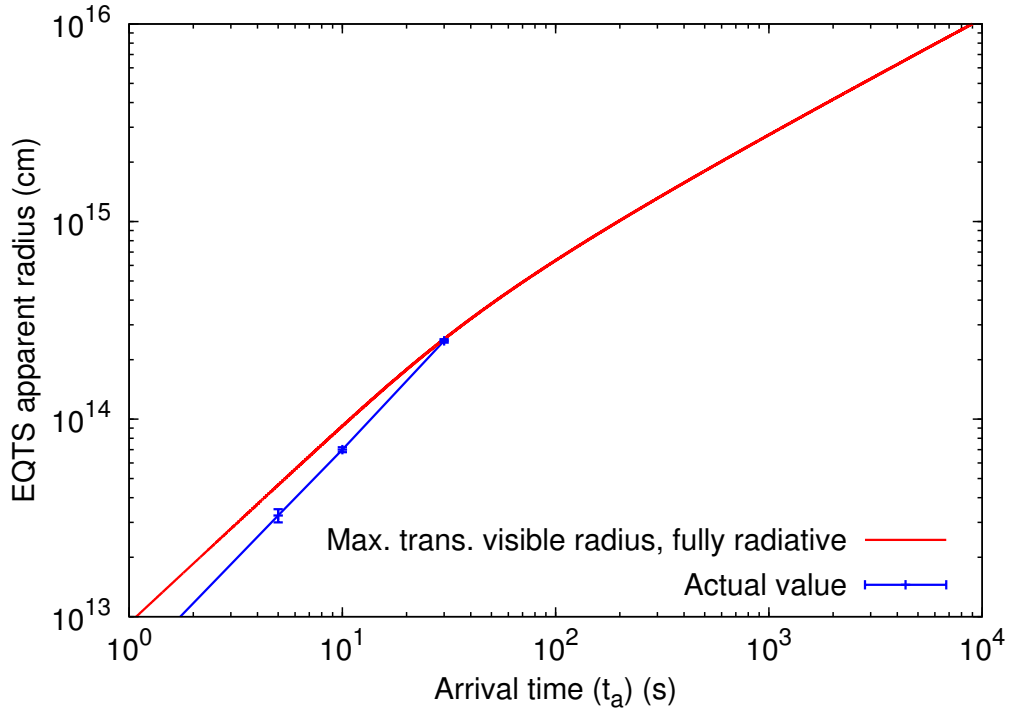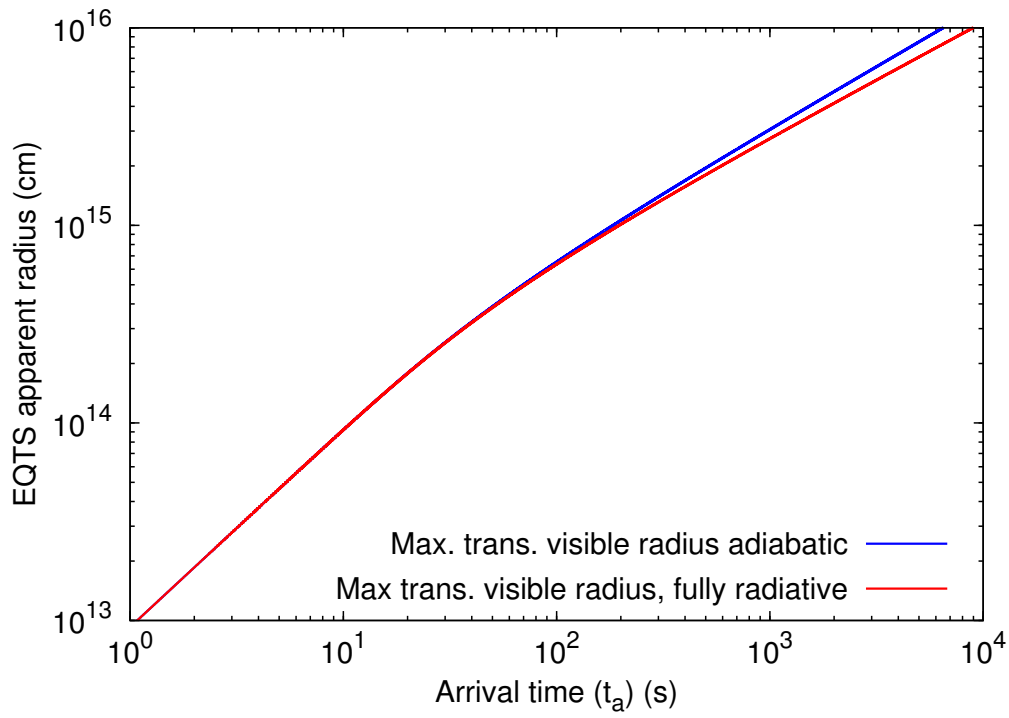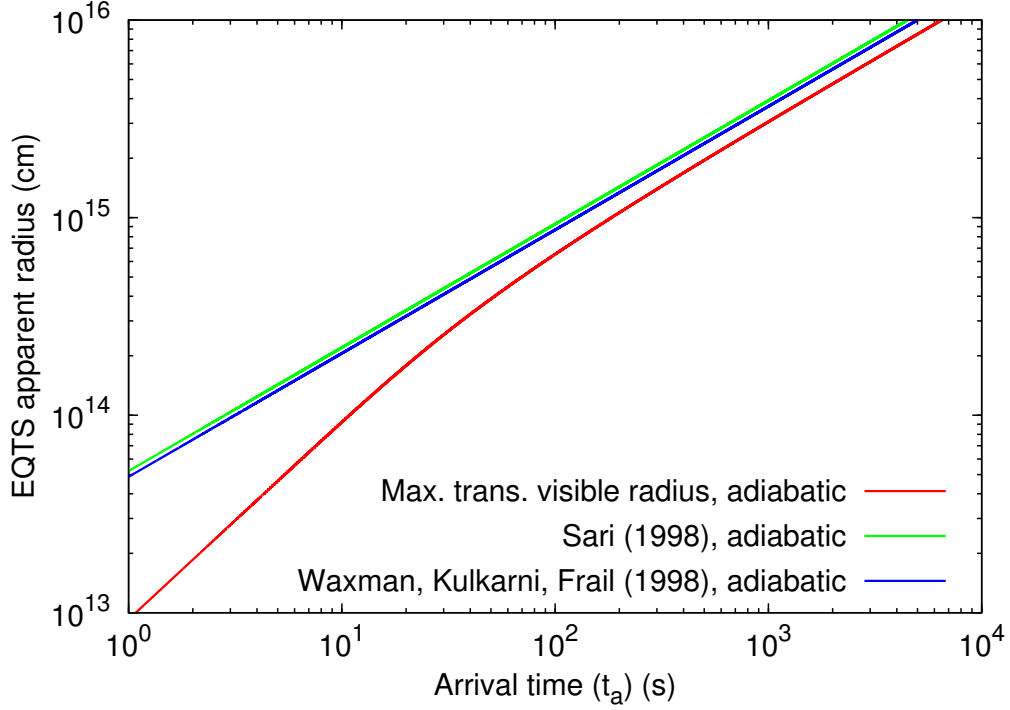
Figure B.3.: The EQTS apparent radius in the sky as a function of the arrival time t_a in the adiabatic regime. The red line represents the maximum transverse EQTS visible radius $r_\perp$ following Eq.(B.0.2). The green line represents Eq.(B.0.3) proposed by Sari (1998). The blue line represents the corresponding modification in the numerical factor proposed by Waxman et al. (1998). These last two lines are almost coincident on the scale of this plot.

approximation implied by Eq.(B.0.3) can therefore be even worse that what represented in Fig. B.3.

B.1. Conclusions

We derived an exact analytic expression for the maximum transverse EQTS visible radius $r_\perp$, both in the fully radiative and in the adiabatic conditions, and we compared it with the approximate formulas commonly used in the current literature in the adiabatic case. We found that these last ones can not be applied in the prompt emission nor in the early afterglow phases. Even when the asymptotic regime is reached ($t_a \gtrsim 10^3$ s), it is necessary a correction to the numerical factor in front of the expression given in Eq.(B.0.3) which should be $\sim 3.1 \times 10^{16}$ instead of 3.91×10^{16} or 3.66×10^{16}.

C. Exact versus approximate solutions in Gamma-Ray Burst afterglows

The consensus has been reached that the afterglow emission originates from a relativistic thin shell of baryonic matter propagating in the CBM and that its description can be obtained from the relativistic conservation laws of energy and momentum. In both our approach and in the other ones in the current literature (see e.g. Piran, 1999; Chiang and Dermer, 1999; Ruffini et al., 2003; Bianco and Ruffini, 2005a) such conservations laws are used. The main difference is that in the current literature it is widely adopted an ultra-relativistic approximation, following the Blandford and McKee (1976) self-similar solution, while we use the exact solution of the equations of motion (see the previous report about "Gamma-Ray Bursts"). We here express such equations in a differential formulation which will be most useful in comparing and contrasting our exact solutions with the ones in the current literature.

C.1. Differential formulation of the afterglow dynamics equations

We recall from the previous report about "Gamma-Ray Bursts"that the relativistic conservation laws of energy and momentum lead to the following finite difference expression for the equations of the afterglow dynamics:

$$\Delta E_{\mathrm{int}} = \rho_{B_1} V_1 \sqrt{1 + 2\gamma_1 \frac{\Delta M_{\mathrm{cbm}} c^2}{\rho_{B_1} V_1} + \left(\frac{\Delta M_{\mathrm{cbm}} c^2}{\rho_{B_1} V_1}\right)^2} - \rho_{B_1} V_1 \left(1 + \frac{\Delta M_{\mathrm{cbm}} c^2}{\rho_{B_1} V_1}\right),$$

$$\text{(C.1.1)}$$

$$\gamma_2 = \frac{\gamma_1 + \frac{\Delta M_{\mathrm{cbm}} c^2}{\rho_{B_1} V_1}}{\sqrt{1 + 2\gamma_1 \frac{\Delta M_{\mathrm{cbm}} c^2}{\rho_{B_1} V_1} + \left(\frac{\Delta M_{\mathrm{cbm}} c^2}{\rho_{B_1} V_1}\right)^2}}. \qquad \text{(C.1.2)}$$

Under the limit:

$$\frac{\Delta M_{\text{cbm}} c^2}{\rho_{B_1} V_1} \ll 1, \qquad (C.1.3)$$

and performing the following substitutions:

$$\Delta E_{\text{int}} \to dE_{\text{int}}, \quad \gamma_2 - \gamma_1 \to d\gamma, \quad \Delta M_{\text{cbm}} \to dM_{\text{cbm}}, \qquad (C.1.4)$$

Eqs.(C.1.1,C.1.2) are equivalent to:

$$dE_{\text{int}} = (\gamma - 1)\, dM_{\text{cbm}} c^2, \qquad (C.1.5a)$$
$$d\gamma = -\tfrac{\gamma^2 - 1}{M} dM_{\text{cbm}}, \qquad (C.1.5b)$$
$$dM = \tfrac{1-\varepsilon}{c^2} dE_{\text{int}} + dM_{\text{cbm}}, \qquad (C.1.5c)$$
$$dM_{\text{cbm}} = 4\pi m_p n_{\text{cbm}} r^2 dr, \qquad (C.1.5d)$$

where, we recall, E_{int}, γ and M are respectively the internal energy, the Lorentz factor and the mass-energy of the expanding pulse, n_{cbm} is the CBM number density which is assumed to be constant, m_p is the proton mass, ε is the emitted fraction of the energy developed in the collision with the CBM and M_{cbm} is the amount of CBM mass swept up within the radius r: $M_{\text{cbm}} = (4/3)\pi(r^3 - r_\circ^3) m_p n_{\text{cbm}}$, where $r_\circ$ is the starting radius of the baryonic shell.

C.2. The exact analytic solutions

A first integral of these equations has been found in both our work and the current literature (see e.g. Piran, 1999; Chiang and Dermer, 1999; Ruffini et al., 2003; Bianco and Ruffini, 2005a). This leads to expressions for the Lorentz gamma factor as a function of the radial coordinate. In the "fully radiative condition" (i.e. $\varepsilon = 1$) we have:

$$\gamma = \frac{1 + (M_{\text{cbm}}/M_B)\left(1 + \gamma_\circ^{-1}\right)\left[1 + (1/2)\left(M_{\text{cbm}}/M_B\right)\right]}{\gamma_\circ^{-1} + (M_{\text{cbm}}/M_B)\left(1 + \gamma_\circ^{-1}\right)\left[1 + (1/2)\left(M_{\text{cbm}}/M_B\right)\right]}, \qquad (C.2.1)$$

while in the "fully adiabatic condition" (i.e. $\varepsilon = 0$) we have:

$$\gamma^2 = \frac{\gamma_\circ^2 + 2\gamma_\circ \left(M_{\text{cbm}}/M_B\right) + \left(M_{\text{cbm}}/M_B\right)^2}{1 + 2\gamma_\circ \left(M_{\text{cbm}}/M_B\right) + \left(M_{\text{cbm}}/M_B\right)^2}, \qquad (C.2.2)$$

where $\gamma_\circ$ is the initial value of the Lorentz gamma factor of the accelerated baryons at the beginning of the afterglow phase.

A major difference between our treatment and the ones in the current liter-

ature is that we have integrated the above equations analytically. Thus we obtained the explicit analytic form of the equations of motion for the expanding shell in the afterglow for a constant CBM density. For the fully radiative case we have explicitly integrated the differential equation for $r(t)$ in Eq.(C.2.1), recalling that $\gamma^{-2} = 1 - [dr/(cdt)]^2$, where t is the time in the laboratory reference frame. The new explicit analytic solution of the equations of motion we have obtained for the relativistic shell in the entire range from the ultra-relativistic to the non-relativistic regimes is (Bianco and Ruffini, 2005b):

$$t = \frac{M_B - m_i^\circ}{2c\sqrt{C}}(r - r_\circ) + \frac{r_\circ\sqrt{C}}{12cm_i^\circ A^2} \ln\left\{\frac{[A+(r/r_\circ)]^3(A^3+1)}{[A^3+(r/r_\circ)^3](A+1)^3}\right\} - \frac{m_i^\circ r_\circ}{8c\sqrt{C}}$$

$$+ t_\circ + \frac{m_i^\circ r_\circ}{8c\sqrt{C}}\left(\frac{r}{r_\circ}\right)^4 + \frac{r_\circ\sqrt{3C}}{6cm_i^\circ A^2}\left[\arctan\frac{2(r/r_\circ)-A}{A\sqrt{3}} - \arctan\frac{2-A}{A\sqrt{3}}\right] \quad \text{(C.2.3)}$$

where we have $A = \sqrt[3]{(M_B - m_i^\circ)/m_i^\circ}$, $C = M_B{}^2(\gamma_\circ - 1)/(\gamma_\circ + 1)$ and $m_i^\circ = (4/3)\pi m_p n_{\text{cbm}} r_\circ^3$.

Correspondingly, in the adiabatic case we have (Bianco and Ruffini, 2005b):

$$t = \left(\gamma_\circ - \frac{m_i^\circ}{M_B}\right)\frac{r - r_\circ}{c\sqrt{\gamma_\circ^2 - 1}} + \frac{m_i^\circ}{4M_B r_\circ^3}\frac{r^4 - r_\circ^4}{c\sqrt{\gamma_\circ^2 - 1}} + t_\circ . \quad \text{(C.2.4)}$$

C.3. Approximations adopted in the current literature

We turn now to the comparison of the exact solutions given in Eqs.(C.2.3) with the approximations used in the current literature. We show that such an approximation holds only in a very limited range of the physical and astrophysical parameters and in an asymptotic regime which is reached only for a very short time, if any, and that therefore it cannot be used for modeling GRBs. Following Blandford and McKee (1976), a so-called "ultrarelativistic" approximation $\gamma_\circ \gg \gamma \gg 1$ has been widely adopted to solve Eqs.(C.1.5) (see e.g. Sari, 1997, 1998; Waxman, 1997; Rees and Meszaros, 1998; Granot et al., 1999a; Panaitescu and Meszaros, 1998; Panaitescu and Mészáros, 1999; Chiang and Dermer, 1999; Piran, 1999; Gruzinov and Waxman, 1999; van Paradijs et al., 2000; Mészáros, 2002, and references therein). This leads to simple constant-index power-law relations:

$$\gamma \propto r^{-a} , \quad \text{(C.3.1)}$$

with $a = 3$ in the fully radiative case and $a = 3/2$ in the fully adiabatic case.

We address now the issue of establishing the domain of applicability of the

simplified Eq.(C.3.1) used in the current literature both in the fully radiative and adiabatic cases.

C.3.1. The fully radiative case

We first consider the fully radiative case. If we assume:

$$1/\left(\gamma_\circ + 1\right) \ll M_{\text{cbm}}/M_B \ll \gamma_\circ/\left(\gamma_\circ + 1\right) < 1, \tag{C.3.2}$$

we have that in the numerator of Eq.(C.2.1) the linear term in M_{cbm}/M_B is negligible with respect to 1 and the quadratic term is *a fortiori* negligible, while in the denominator the linear term in M_{cbm}/M_B is the leading one. Eq.(C.2.1) then becomes:

$$\gamma \simeq \left[\gamma_\circ/\left(\gamma_\circ + 1\right)\right] M_B/M_{\text{cbm}}. \tag{C.3.3}$$

If we multiply the terms of Eq.(C.3.2) by $(\gamma_\circ + 1)/\gamma_\circ$, we obtain $1/\gamma_\circ \ll (M_{\text{cbm}}/M_B)[(\gamma_\circ + 1)/\gamma_\circ] \ll 1$, which is equivalent to:

$$\gamma_\circ \gg \left[\gamma_\circ/(\gamma_\circ + 1)\right](M_B/M_{\text{cbm}}) \gg 1, \tag{C.3.4}$$

or, using Eq.(C.3.3), to:

$$\gamma_\circ \gg \gamma \gg 1, \tag{C.3.5}$$

which is indeed the inequality adopted in the "ultrarelativistic" approximation in the current literature. If we further assume $r^3 \gg r_\circ^3$, Eq.(C.3.3) can be approximated by a simple constant-index power-law as in Eq.(C.3.1):

$$\gamma \simeq \left[\gamma_\circ/\left(\gamma_\circ + 1\right)\right] M_B/\left[(4/3)\,\pi n_{\text{cbm}} m_p r^3\right] \propto r^{-3}. \tag{C.3.6}$$

We turn now to the range of applicability of these approximations, consistently with the inequalities given in Eq.(C.3.2). It then becomes manifest that these inequalities can only be enforced in a finite range of M_{cbm}/M_B. The lower limit (LL) and the upper limit (UL) of such range can be conservatively estimated:

$$\left(\frac{M_{\text{cbm}}}{M_B}\right)_{LL} = 10^2 \frac{1}{\gamma_\circ + 1}, \quad \left(\frac{M_{\text{cbm}}}{M_B}\right)_{UL} = 10^{-2} \frac{\gamma_\circ}{\gamma_\circ + 1}. \tag{C.3.7a}$$

The allowed range of variability, if it exists, is then given by:

$$\left(\frac{M_{\text{cbm}}}{M_B}\right)_{UL} - \left(\frac{M_{\text{cbm}}}{M_B}\right)_{LL} = 10^{-2} \frac{\gamma_\circ - 10^4}{\gamma_\circ + 1} > 0. \tag{C.3.7b}$$

A necessary condition for the applicability of the above approximations is

therefore:

$$\gamma_\circ > 10^4 \,. \tag{C.3.8}$$

It is important to emphasize that Eq.(C.3.8) is only a *necessary* condition for the applicability of the approximate Eq.(C.3.6) but it is not *sufficient*: Eq.(C.3.6) in fact can be applied only in the very limited range of *r* values whose upper and lower limits are given in Eq.(C.3.7a). See for explicit examples section C.4 below.

C.3.2. The adiabatic case

We now turn to the adiabatic case. If we assume:

$$1/(2\gamma_\circ) \ll M_{\mathrm{cbm}}/M_B \ll \gamma_\circ/2 \,, \tag{C.3.9}$$

we have that in the numerator of Eq.(C.2.2) all terms are negligible with respect to $\gamma_\circ^2$, while in the denominator the leading term is the linear one in M_{cbm}/M_B. Eq.(C.2.2) then becomes:

$$\gamma \simeq \sqrt{(\gamma_\circ/2)\,M_B/M_{\mathrm{cbm}}} \,. \tag{C.3.10}$$

If we multiply the terms of Eq.(C.3.9) by $2/\gamma_\circ$, we obtain:

$$1/\gamma_\circ^2 \ll (2/\gamma_\circ)(M_{\mathrm{cbm}}/M_B) \ll 1 \,, \tag{C.3.11}$$

which is equivalent to $\gamma_\circ^2 \gg (\gamma_\circ/2)(M_B/M_{\mathrm{cbm}}) \gg 1$, or, using Eq.(C.3.10), to:

$$\gamma_\circ^2 \gg \gamma^2 \gg 1 \,. \tag{C.3.12}$$

If we now further assume $r^3 \gg r_\circ^3$, Eq.(C.3.10) can be approximated by a simple constant-index power-law as in Eq.(C.3.1):

$$\gamma \simeq \sqrt{(\gamma_\circ/2)\,M_B/\left[(4/3)\,\pi n_{\mathrm{cbm}}m_p r^3\right]} \propto r^{-3/2} \,. \tag{C.3.13}$$

We turn now to the range of applicability of these approximations, consistently with the inequalities given in Eq.(C.3.9). It then becomes manifest that these inequalities can only be enforced in a finite range of M_{cbm}/M_B. The lower limit (LL) and the upper limit (UL) of such range can be conservatively estimated:

$$\left(\frac{M_{\mathrm{cbm}}}{M_B}\right)_{LL} = 10^2 \frac{1}{2\gamma_\circ} \,, \quad \left(\frac{M_{\mathrm{cbm}}}{M_B}\right)_{UL} = 10^{-2} \frac{\gamma_\circ}{2} \,. \tag{C.3.14a}$$
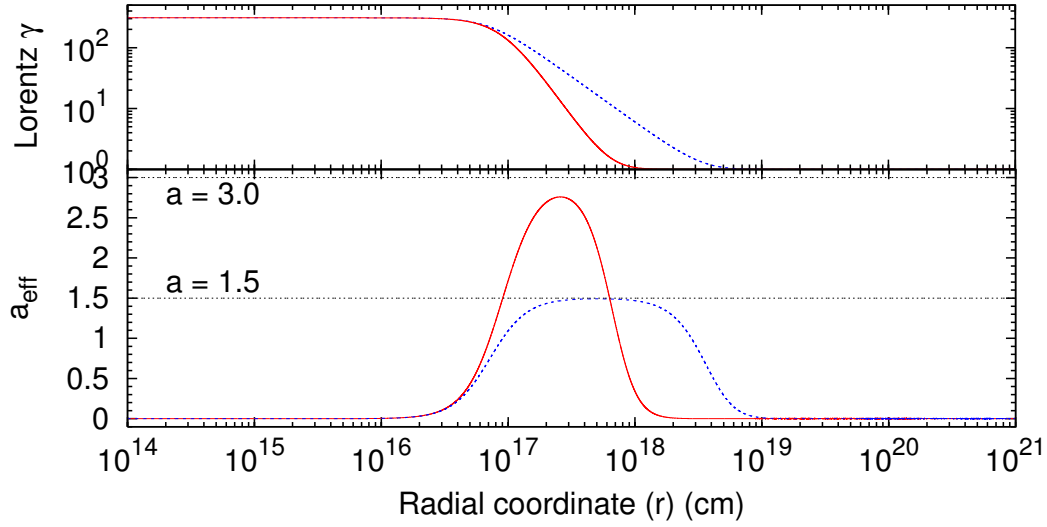
Figure C.1.: In the upper panel, the analytic behavior of the Lorentz γ factor during the afterglow era is plotted versus the radial coordinate of the expanding thin baryonic shell in the fully radiative case of GRB 991216 (solid red line) and in the adiabatic case starting from the same initial conditions (dotted blue line). In the lower panel are plotted the corresponding values of the "effective" power-law index a_{eff} (see Eq.(C.4.1)), which is clearly not constant, is highly varying and systematically lower than the constant values 3 and 3/2 purported in the current literature (horizontal dotted black lines). Details in Bianco and Ruffini (2005a).

The allowed range of variability, if it exists, is then given by:

$$\left(\frac{M_{cbm}}{M_B}\right)_{UL} - \left(\frac{M_{cbm}}{M_B}\right)_{LL} = 10^{-2}\frac{\gamma_\circ^2 - 10^4}{2\gamma_\circ} > 0. \qquad \text{(C.3.14b)}$$

A necessary condition for the applicability of the above approximations is therefore:

$$\gamma_\circ > 10^2. \qquad \text{(C.3.15)}$$

Again, it is important to emphasize that Eq.(C.3.15) is only a *necessary* condition for the applicability of the approximate Eq.(C.3.13), but it is not *sufficient*: Eq.(C.3.13) in fact can be applied only in the very limited range of r values whose upper and lower limits are given in Eq.(C.3.14a). See for explicit examples section C.4 below.

C.4. A specific example

Having obtained the analytic expression of the Lorentz gamma factor for the fully radiative case in Eq.(C.2.1), we illustrate in Fig. C.1 the corresponding gamma factor as a function of the radial coordinate in the afterglow phase for GRB 991216 (see Ruffini et al., 2003, and references therein). We have also represented the corresponding solution which can be obtained in the adiabatic case, using Eq.(C.2.2), starting from the same initial conditions. It is clear that in both cases there is not a simple power-law relation like Eq.(C.3.1) with a constant index a. We can at most define an "instantaneous" value a_{eff} for an "effective" power-law behavior:

$$a_{eff} = -\frac{d\ln\gamma}{d\ln r}. \tag{C.4.1}$$

Such an "effective" power-law index of the exact solution smoothly varies from 0 to a maximum value which is always smaller than 3 or 3/2, in the fully radiative and adiabatic cases respectively, and finally decreases back to 0 (see Fig. C.1). We see in particular, from Fig. C.1, how in the fully radiative case the power-law index is consistently smaller than 3, and in the adiabatic case $a_{eff} = 3/2$ is approached only for a small interval of the radial coordinate corresponding to the latest parts of the afterglow with a Lorentz gamma factor of the order of 10. In this case of GRB 991216 we have, in fact, $\gamma_\circ = 310.13$ and neither Eq.(C.3.5) nor Eq.(C.3.12) can be satisfied for any value of r. Therefore, neither in the fully radiative nor in the adiabatic case the constant-index power-law expression in Eq.(C.3.1) can be applied.

For clarity, we have integrated in Fig. C.2 an ideal GRB afterglow with the initial conditions as GRB 991216 for selected higher values of the initial Lorentz gamma factor: $\gamma_\circ = 10^3, 10^5, 10^7, 10^9$. For $\gamma_\circ = 10^3$, we then see that, again, in the fully radiative condition $a_{eff} = 3$ is never reached and in the adiabatic case $a_{eff} \simeq 3/2$ only in the region where $10 < \gamma < 50$. Similarly, for $\gamma_\circ = 10^5$, in the fully radiative case $a_{eff} \simeq 3$ is only reached around the point $\gamma = 10^2$, and in the adiabatic case $a_{eff} \simeq 3/2$ for $10 < \gamma < 10^2$, although the non-power-law behavior still remains in the early and latest afterglow phases corresponding to the $\gamma \equiv \gamma_\circ$ and $\gamma \to 1$ regimes. The same conclusion can be reached for the remaining cases $\gamma_\circ = 10^7$ and $\gamma_\circ = 10^9$.

We like to emphasize that the early part of the afterglow, where $\gamma \equiv \gamma_\circ$, which cannot be described by the constant-index power-law approximation, do indeed corresponds to the rising part of the afterglow bolometric luminosity and to its peak, which is reached as soon as the Lorentz gamma factor starts to decrease. We have shown (see e.g. Ruffini et al., 2001a, 2003, 2005, and references therein) how the correct identifications of the raising part and
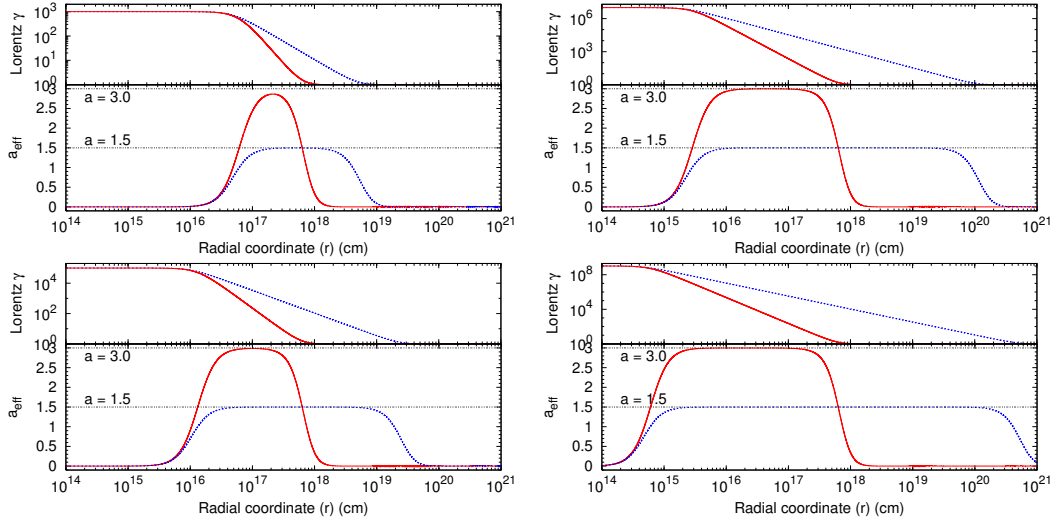
Figure C.2.: In these four diagrams we reproduce the same quantities plotted in Fig. C.1 for four higher values of $\gamma_\circ$. The upper (lower) left diagram corresponds to $\gamma_\circ = 10^3$ ($\gamma_\circ = 10^5$). The upper (lower) right diagram corresponds to $\gamma_\circ = 10^7$ ($\gamma_\circ = 10^9$). It is manifest how asymptotically, by increasing the value of $\gamma_\circ$, the values $a = 3$ and $a = 3/2$ (horizontal black dotted lines) are reached, but only in a limited range of the radial co-ordinate and anyway for values of $\gamma_\circ$ much larger than the ones actually observed in GRBs. Details in Bianco and Ruffini (2005a).

the peak of the afterglow are indeed crucial for the explanation of the observed "prompt radiation". Similarly, the power-law cannot be applied during the entire approach to the newtonian regime, which corresponds to some of the actual observations occurring in the latest afterglow phases.

D. Exact analytic expressions for the equitemporal surfaces in Gamma-Ray Burst afterglows

D.1. The definition of the EQTSs

For a relativistically expanding spherically symmetric source the "equitemporal surfaces" (EQTSs, namely the locus of source points of the signals arriving at the observer at the same time) are surfaces of revolution about the line of sight. The general expression for their profile, in the form $\vartheta = \vartheta(r)$, corresponding to an arrival time t_a of the photons at the detector, can be obtained from (see e.g. Ruffini et al., 2003; Bianco and Ruffini, 2004, 2005b, and Figs. D.1–D.4):

$$ct_a = ct(r) - r\cos\vartheta + r^\star, \tag{D.1.1}$$

where $r^\star$ is the initial size of the expanding source, ϑ is the angle between the radial expansion velocity of a point on its surface and the line of sight, and $t = t(r)$ is its equation of motion, expressed in the laboratory frame, obtained by the integration of Eqs.(C.1.5). From the definition of the Lorentz gamma factor $\gamma^{-2} = 1 - (dr/cdt)^2$, we have in fact:

$$ct(r) = \int_0^r \left[1 - \gamma^{-2}(r')\right]^{-1/2} dr', \tag{D.1.2}$$

where $\gamma(r)$ comes from the integration of Eqs.(C.1.5).

It is appropriate to underline a basic difference between the apparent superluminal velocity orthogonal to the line of sight, $v^\perp \simeq \gamma v$, and the apparent superluminal velocity along the line of sight, $v^\parallel \simeq \gamma^2 v$. In the case of GRBs, this last one is the most relevant: for a Lorentz gamma factor $\gamma \simeq 300$ we have $v^\parallel \simeq 10^5 c$. This is self-consistently verified in the structure of the "prompt radiation" of GRBs (see e.g. Ruffini et al., 2002).
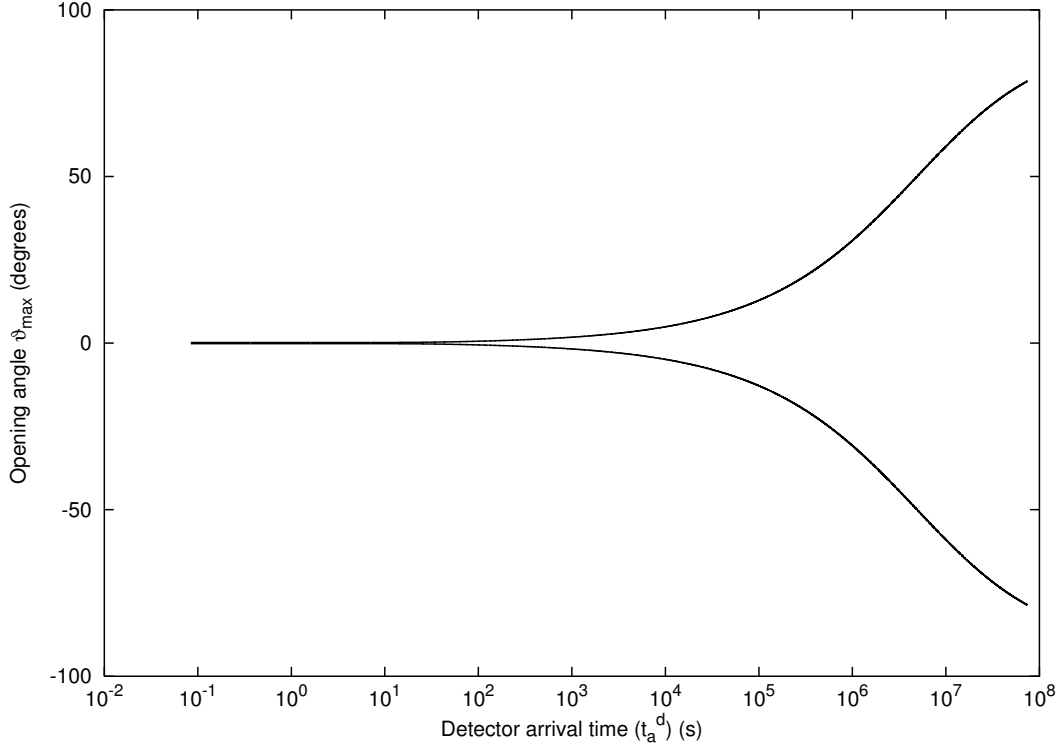
Figure D.1.: Not all values of ϑ are allowed. Only photons emitted at an angle such that $\cos \vartheta \geq (v/c)$ can be viewed by the observer. Thus the maximum allowed ϑ value ϑ_{max} corresponds to $\cos \vartheta_{max} = (v/c)$. In this figure we show ϑ_{max} (i.e. the angular amplitude of the visible area of the ABM pulse) in degrees as a function of the arrival time at the detector for the photons emitted along the line of sight (see text). In the earliest GRB phases $v \sim c$ and so $\vartheta_{max} \sim 0$. On the other hand, in the latest phases of the afterglow the ABM pulse velocity decreases and ϑ_{max} tends to the maximum possible value, i.e. $90°$. Details in Ruffini et al. (2002, 2003).
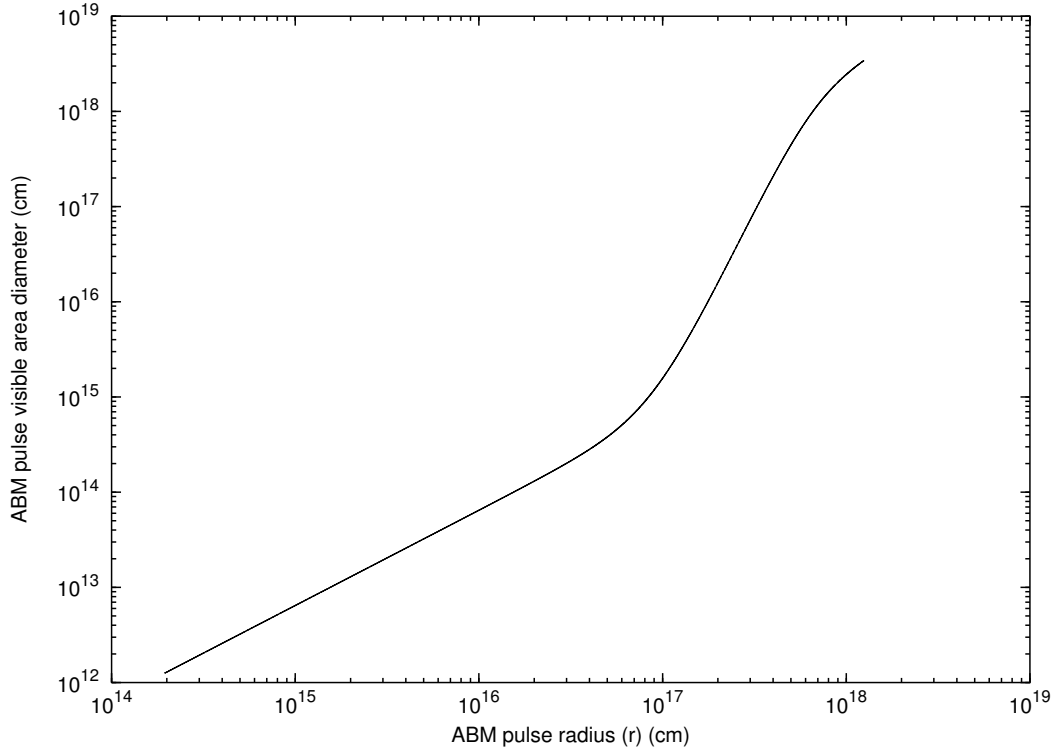
Figure D.2.: The diameter of the visible area is represented as a function of the ABM pulse radius. In the earliest expansion phases ($\gamma \sim 310$) ϑ_{max} is very small (see Fig. D.3), so the visible area is just a small fraction of the total ABM pulse surface. On the other hand, in the final expansion phases $\vartheta_{max} \rightarrow 90°$ and almost all the ABM pulse surface becomes visible. Details in Ruffini et al. (2002, 2003).
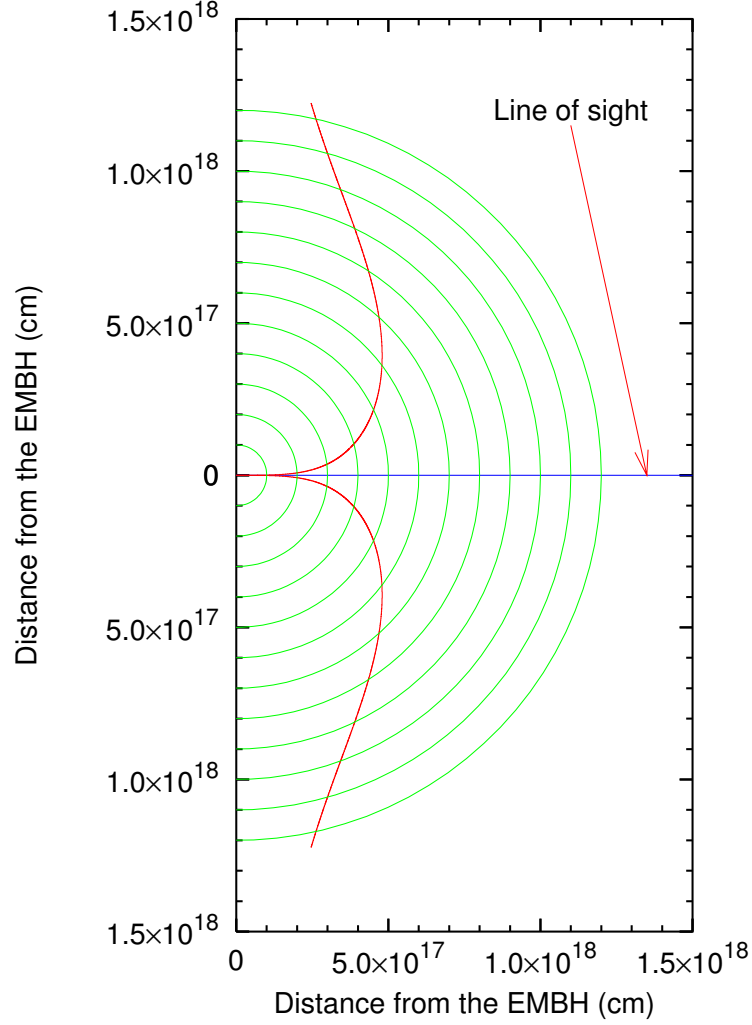
Figure D.3.: This figure shows the temporal evolution of the visible area of the ABM pulse. The green half-circles are the expanding ABM pulse at radii corresponding to different laboratory times. The red curve marks the boundary of the visible region. The black hole is located at position (0,0) in this plot. Again, in the earliest GRB phases the visible region is squeezed along the line of sight, while in the final part of the afterglow phase almost all the emitted photons reach the observer. This time evolution of the visible area is crucial to the explanation of the GRB temporal structure. Details in Ruffini et al. (2002, 2003).
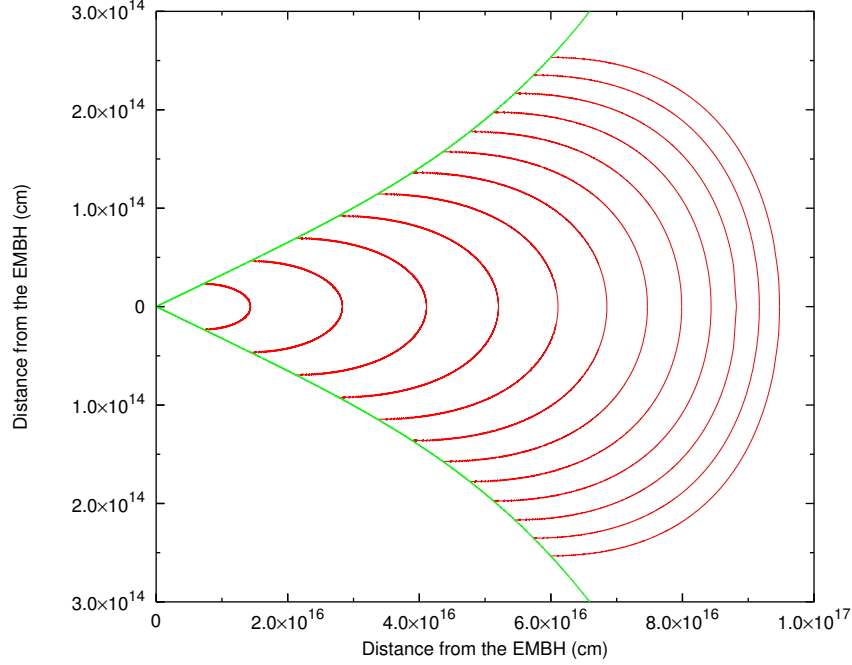
Figure D.4.: Due to the extremely high and extremely varying Lorentz gamma factor, photons reaching the detector on the Earth at the same arrival time are actually emitted at very different times and positions. We represent here the surfaces of photon emission corresponding to selected values of the photon arrival time at the detector: the *equitemporal surfaces* (EQTS). Such surfaces differ from the ellipsoids described by Rees in the context of the expanding radio sources with typical Lorentz factor $\gamma \sim 4$ and constant (see Rees, 1966). In fact, in GRB 991216 the Lorentz gamma factor ranges from 310 to 1. The EQTSs represented here (red lines) correspond respectively to values of the arrival time ranging from $5\,s$ (the smallest surface on the left of the plot) to $60\,s$ (the largest one on the right) in the case of GRB 991216. Each surface differs from the previous one by $5\,s$. To each EQTS contributes emission processes occurring at different values of the Lorentz gamma factor. The green lines are the boundaries of the visible area of the ABM pulse and the black hole is located at position $(0, 0)$ in this plot. Note the different scales on the two axes, indicating the very high EQTS "effective eccentricity". The time interval from 5 s to 60 s has been chosen to encompass the E-APE emission, ranging from $\gamma = 308.8$ to $\gamma = 56.84$. Details in Ruffini et al. (2002, 2003).

D.2. The analytic expressions for the EQTSes

D.2.1. The fully radiative case

The analytic expression for the EQTS in the fully radiative regime can then be obtained substituting $t(r)$ from Eq.(C.2.3) in Eq.(D.1.1) (see Bianco and Ruffini, 2005b). We obtain:

$$
\cos \vartheta = \frac{M_B - m_i^\circ}{2r\sqrt{C}} (r - r_\circ) + \frac{m_i^\circ r_\circ}{8r\sqrt{C}} \left[\left(\frac{r}{r_\circ} \right)^4 - 1 \right]
$$

$$
+ \frac{r_\circ \sqrt{C}}{12 r m_i^\circ A^2} \ln \left\{ \frac{[A + (r/r_\circ)]^3 (A^3 + 1)}{\left[A^3 + (r/r_\circ)^3 \right] (A + 1)^3} \right\} + \frac{ct_\circ}{r} - \frac{ct_a}{r}
$$

$$
+ \frac{r^\star}{r} + \frac{r_\circ \sqrt{3C}}{6 r m_i^\circ A^2} \left[\arctan \frac{2(r/r_\circ) - A}{A\sqrt{3}} - \arctan \frac{2 - A}{A\sqrt{3}} \right] , \tag{D.2.1}
$$

where A, C and m_i° are the same as in Eq.(C.2.3).

D.2.2. The adiabatic case

The analytic expression for the EQTS in the adiabatic regime can then be obtained substituting $t(r)$ from Eq.(C.2.4) in Eq.(D.1.1) (see Bianco and Ruffini, 2005b). We obtain:

$$
\cos \vartheta = \frac{m_i^\circ}{4 M_B \sqrt{\gamma_\circ^2 - 1}} \left[\left(\frac{r}{r_\circ} \right)^3 - \frac{r_\circ}{r} \right] + \frac{ct_\circ}{r}
$$

$$
- \frac{ct_a}{r} + \frac{r^\star}{r} - \frac{\gamma_\circ - (m_i^\circ / M_B)}{\sqrt{\gamma_\circ^2 - 1}} \left[\frac{r_\circ}{r} - 1 \right] . \tag{D.2.2}
$$

D.2.3. Comparison between the two cases

The two EQTSs are represented at selected values of the arrival time t_a in Fig. D.5, where the illustrative case of GRB 991216 has been used as a prototype. The initial conditions at the beginning of the afterglow era are in this case given by $\gamma_\circ = 310$, $r_\circ = 1.94 \times 10^{14}$ cm, $t_\circ = 6.48 \times 10^3$ s, $r^\star = 2.35 \times 10^8$ cm (see Ruffini et al., 2001b,a, 2002, 2003; Bianco and Ruffini, 2005b).
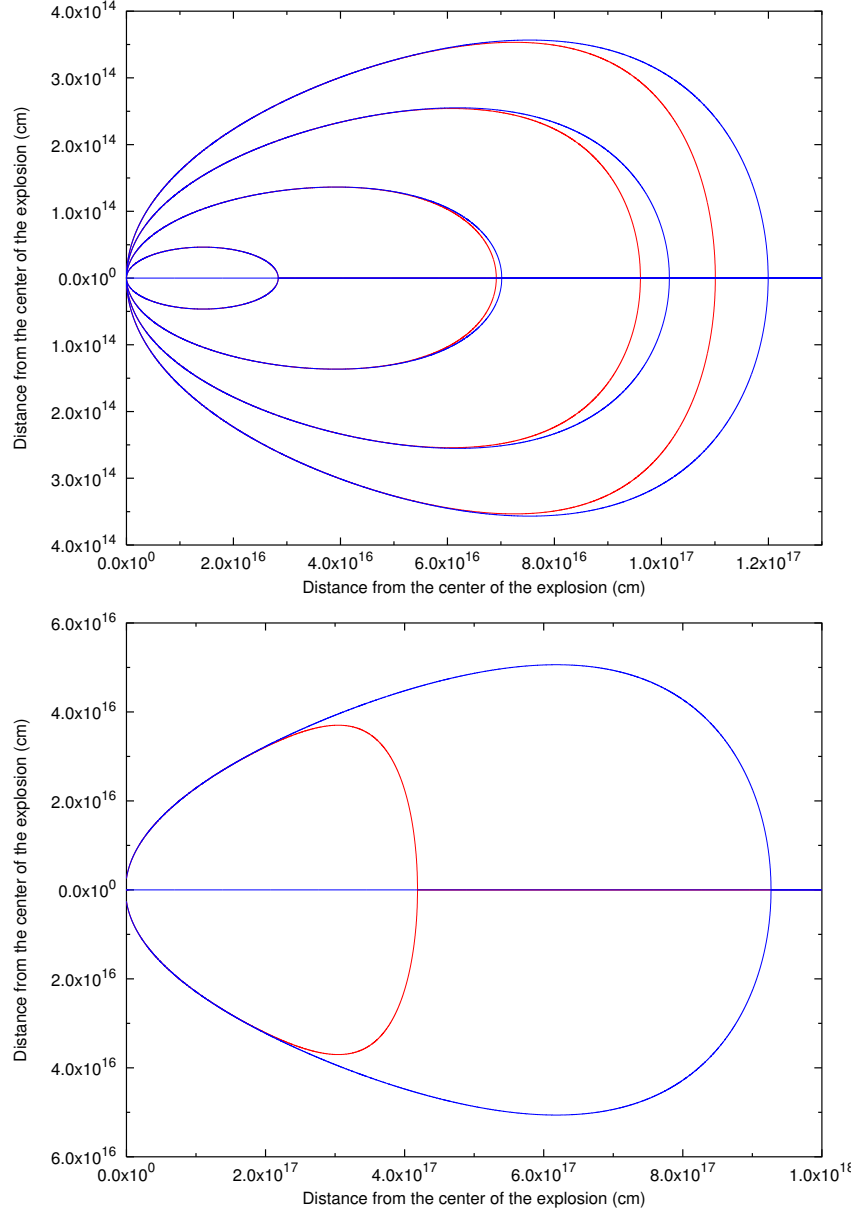
Figure D.5.: Comparison between EQTSs in the adiabatic regime (blue lines) and in the fully radiative regime (red lines). The upper plot shows the EQTSs for $t_a = 5$ s, $t_a = 15$ s, $t_a = 30$ s and $t_a = 45$ s, respectively from the inner to the outer one. The lower plot shows the EQTS at an arrival time of 2 days. Details in Bianco and Ruffini (2005b).

D.3. Approximations adopted in the current literature

In the current literature two different treatments of the EQTSs exist: one by Panaitescu and Meszaros (1998) and one by Sari (1998) later applied also by Granot et al. (1999a) (see also Piran, 1999, 2000; van Paradijs et al., 2000, and references therein).

In both these treatments, instead of the more precise dynamical equations given in Eqs.(C.2.2,C.2.1), the simplified formula, based on the "ultrarelativistic" approximation, given in Eq.(C.3.1) has been used. A critical analysis comparing and contrasting our exact solutions with Eq.(C.3.1) has been presented in the previous section and in Bianco and Ruffini (2005a). As a further approximation, instead of the exact Eq.(D.1.2), they both use the following expansion at first order in γ^{-2}:

$$ct(r) = \int_0^r \left[1 + \frac{1}{2\gamma^2(r')} \right] dr'. \tag{D.3.1}$$

Correspondingly, instead of the exact Eq.(C.2.4) and Eq.(C.2.3), they find:

$$t(r) = \frac{r}{c} \left[1 + \frac{1}{2(2a+1)\gamma^2(r)} \right], \tag{D.3.2a}$$

$$t(r) = \frac{r}{c} \left[1 + \frac{1}{16\gamma^2(r)} \right]. \tag{D.3.2b}$$

The first expression has been given by Panaitescu and Meszaros (1998) and applies both in the adiabatic ($a = 3/2$) and in the fully radiative ($a = 3$) cases (see their Eq.(2)). The second one has been given by Sari (1998) in the adiabatic case (see his Eq.(2)). Note that the first expression, in the case $a = 3/2$, does not coincide with the second one: Sari (1998) uses a Lorentz gamma factor Γ of a shock front propagating in the expanding pulse, with $\Gamma = \sqrt{2}\gamma$.

Instead of the exact Eqs.(D.1.1), Panaitescu and Meszaros (1998) and Sari (1998) both uses the following equation:

$$ct_a = ct(r) - r\cos\vartheta, \tag{D.3.3}$$

where the initial size $r^\star$ has been neglected. The following approximate ex-

pressions for the EQTSs have been then presented:

$$\vartheta = 2\arcsin\left[\frac{1}{2\gamma_\circ}\sqrt{\frac{2\gamma_\circ^2 c t_a}{r} - \frac{1}{2a+1}\left(\frac{r}{r_\circ}\right)^{2a}}\right], \quad (D.3.4a)$$

$$\cos\vartheta = 1 - \frac{1}{16\gamma_L^2}\left[\left(\frac{r}{r_L}\right)^{-1} - \left(\frac{r}{r_L}\right)^3\right]. \quad (D.3.4b)$$

The first expression has been given by Panaitescu and Meszaros (1998) and applies both in the adiabatic ($a = 3/2$) and in the fully radiative ($a = 3$) cases (see their Eq.(3)). The second expression, where $\gamma_L \equiv \gamma(\vartheta = 0)$ over the given EQTS and $r_L = 16\gamma_L^2 c t_a$, has been given by Sari (1998) in the adiabatic case (see his Eq.(5)).

Without entering into the relative merit of such differing approaches, we show in Figs. D.6–D.7 that both of them lead to results different from the ones computed with the exact solutions. The consequences of using the approximate formula given in Eq.(C.3.1) to compute the expression $t \equiv t(r)$, instead of the exact solution of Eqs.(C.1.5), are clearly shown in Figs. D.6–D.7. The EQTSs represented in these figures are computed at selected values of the detector arrival time both in the early (~ 35 s) and in the late (~ 4 day) phases of the afterglow. Both the fully radiative and fully adiabatic cases are examined. Note the approximate expression of the EQTS can only be defined for $\gamma < \gamma_d$ and $r > r_d$ (see Bianco and Ruffini, 2005b). Consequently, at $t_a^d = 35$ s the approximate EQTSs are represented by arcs, markedly different from the exact solution (see the upper panels of Figs. D.6–D.7). The same conclusion is found for the EQTS at $t_a^d = 4$ days, where marked differences are found both for the fully radiative and adiabatic regimes (see the lower panels of Figs. D.6–D.7).
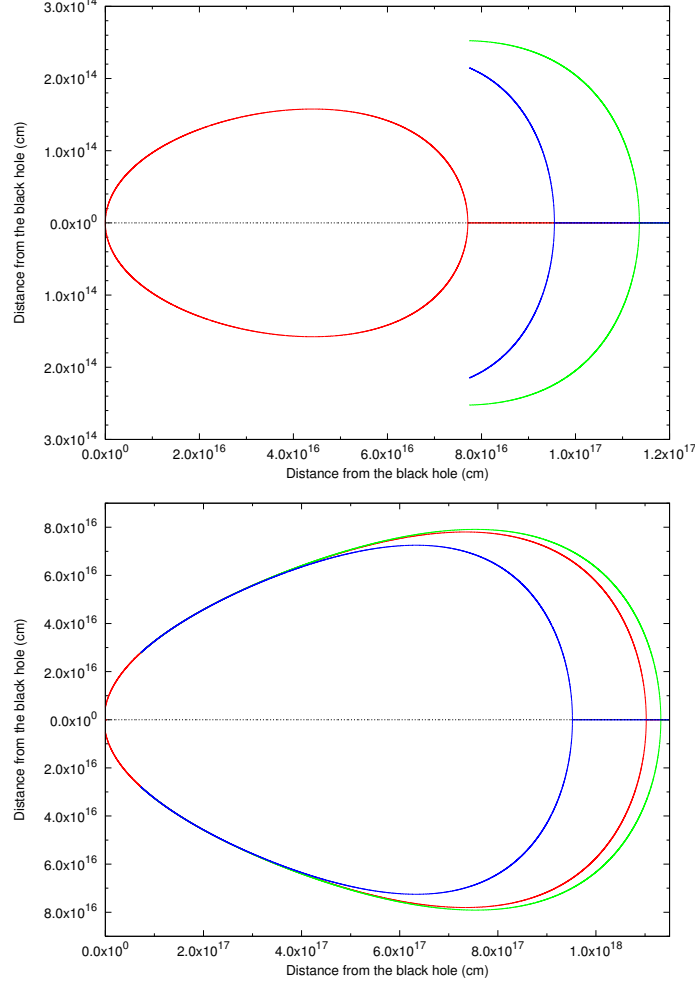
Figure D.6.: Comparison between the EQTSs computed using the approximate formulas given by Panaitescu and Meszaros (1998) (blue line) and by Sari (1998); Granot et al. (1999a) (green line) in the fully adiabatic case ($a = 3/2$ in Eqs.(D.3.4)) and the corresponding ones computed using the exact analytic expression given in Eq.(D.2.2) (red line). The difference between the green line and the blue line is due to the factor $\sqrt{2}$ in the Lorentz γ factor adopted by Sari (see text). The upper (lower) panel corresponds to $t_a^d = 35$ s ($t_a^d = 4$ day). The approximate curves are not drawn entirely because Eqs.(D.3.4) are declared to be valid only where $\gamma < 2/3\gamma_\circ$. Details in Bianco and Ruffini (2004, 2005b).

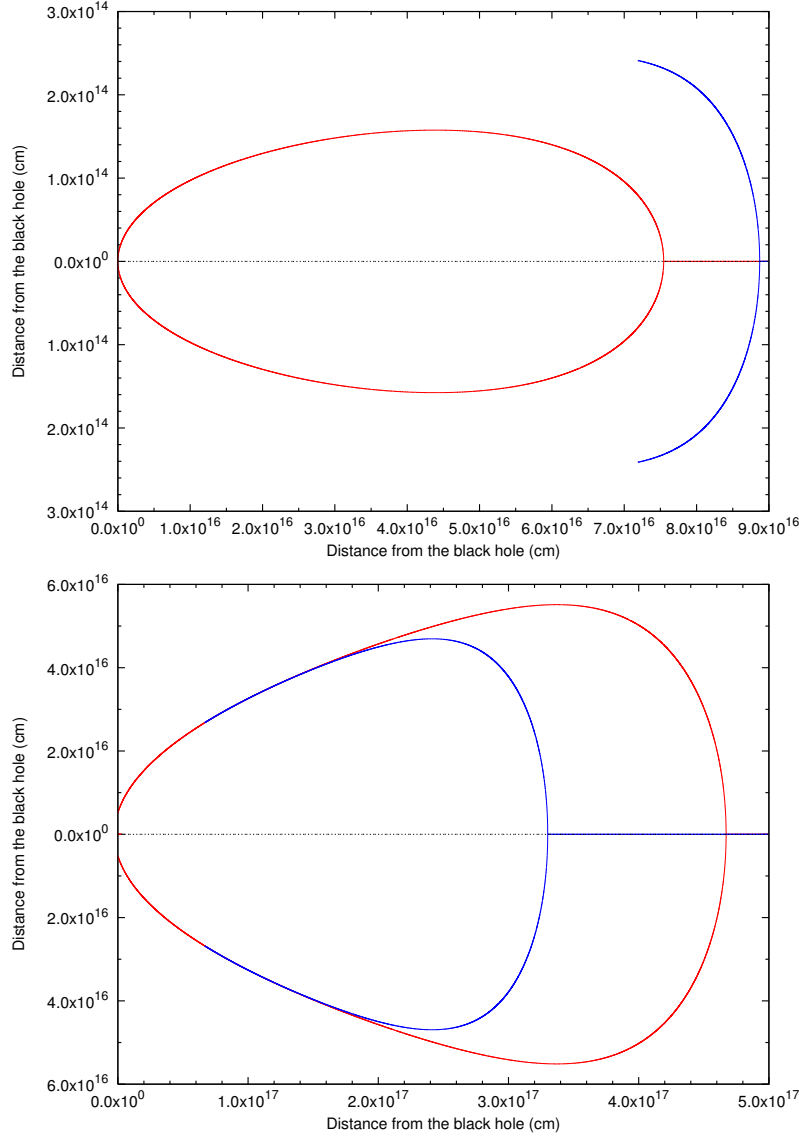**Figure D.7.:** Comparison between the EQTSs computed using the approximate formulas given by Panaitescu and Meszaros (1998) (blue line) in the fully radiative case ($a = 3$ in the first of Eqs.(D.3.4)) and the corresponding ones computed using the exact analytic expression given in Eq.(D.2.1) (red line). The upper (lower) panel corresponds to $t_a^d = 35$ s ($t_a^d = 4$ day). Details in Bianco and Ruffini (2004, 2005b).

E. Exact versus approximate beaming formulas in Gamma-Ray Burst afterglows

Using the exact solutions introduced in the previous sections, we here introduce the exact analytic expressions of the relations between the detector arrival time t_a^d of the GRB afterglow radiation and the corresponding half-opening angle ϑ of the expanding source visible area due to the relativistic beaming (see e.g. Ruffini et al., 2003). Such visible area must be computed not over the spherical surface of the shell, but over the EQuiTemporal Surface (EQTS) of detector arrival time t_a^d, i.e. over the surface locus of points which are source of the radiation reaching the observer at the same arrival time t_a^d (see Bianco and Ruffini, 2004, 2005b, for details). The exact analytic expressions for the EQTSs in GRB afterglows, which have been presented in Eqs.(D.2.2)–(D.2.1) and in Bianco and Ruffini (2005b), are therefore crucial in our present derivation. This approach clearly differs from the ones in the current literature, which usually neglect the contributions of the radiation emitted from the entire EQTS.

The analytic relations between t_a^d and ϑ presented in this section allow to compute, assuming that the expanding shell is not spherically symmetric but is confined into a narrow jet with half-opening angle $\vartheta_\circ$, the value $(t_a^d)_{jet}$ of the detector arrival time at which we start to "see" the sides of the jet. A corresponding "break" in the observed light curve should occur later than $(t_a^d)_{jet}$ (seee.g. Sari et al., 1999). In the current literature, $(t_a^d)_{jet}$ is usually defined as the detector arrival time at which $\gamma \sim 1/\vartheta_\circ$, where γ is the Lorentz factor of the expanding shell (see e.g. Sari et al., 1999, and also our Eq.(E.1.2) below). In our formulation we do not consider effects of lateral spreadings of the jet.

In the current literature, in the case of adiabatic regime, different approximate power-law relations between $(t_a^d)_{jet}$ and $\vartheta_\circ$ have been presented, in contrast to each other (see e.g. Sari et al., 1999; Panaitescu and Mészáros, 1999; Panaitescu, 2006). We show here that in four specific cases of GRBs, encompassing more than 5 orders of magnitude in energy and more than 2 orders of magnitude in CBM density, both the one by Panaitescu and Mészáros (1999) and the one by Sari et al. (1999) overestimate the exact analytic result. A third

relation just presented by Panaitescu (2006) slightly underestimate the exact analytic result. We also present an empirical fit of the numerical solutions of the exact equations for the adiabatic regime, compared and contrasted with the three above approximate relations. In the fully radiative regime, and therefore in the general case, no simple power-law relation of the kind found in the adiabatic regime can be established and the general approach we have outlined has to be followed.

Although evidence for spherically symmetric emission in GRBs is emerging from observations (Sakamoto et al., 2006) and from theoretical argumentations (Ruffini et al., 2004b, 2006), it is appropriate to develop here an exact theoretical treatment of the relation between $(t_a^d)_{jet}$ and $\vartheta_\circ$. This will allow to make an assessment on the existence and, in the positive case, on the extent of beaming in GRBs, which in turn is going to be essential for establishing their correct energetics.

E.1. Analytic formulas for the beaming angle

The boundary of the visible region of a relativistic thin and uniform shell expanding in the CBM is defined by Ruffini et al. (see e.g. 2003, and references therein):

$$\cos \vartheta = \frac{v}{c}, \tag{E.1.1}$$

where ϑ is the angle between the line of sight and the radial expansion velocity of a point on the shell surface, v is the velocity of the expanding shell and c is the speed of light. To find the value of the half-opening beaming angle $\vartheta_\circ$ corresponding to an observed arrival time $(t_a^d)_{jet}$, this equation must be solved together with the equation describing the EQTS of arrival time $(t_a^d)_{jet}$ (Bianco and Ruffini, 2005b). In other words, we must solve the following system:

$$\begin{cases} \cos \vartheta_\circ &= \frac{v(r)}{c} \\ \cos \vartheta_\circ &= \cos \left\{ \vartheta \left[r; (t_a^d)_{jet}\right] \big|_{EQTS\left[(t_a^d)_{jet}\right]} \right\} \end{cases} . \tag{E.1.2}$$

It should be noted that, in the limit $\vartheta_\circ \to 0$ and $v \to c$, this definition of $(t_a^d)_{jet}$ is equivalent to the one usually adopted in the current literature (see above).

E.1.1. The fully radiative regime

In this case (see Eq.(C.2.1) and Bianco and Ruffini, 2005b,a), the analytic solution of the equations of motion gives:

$$\frac{v}{c} = \frac{\sqrt{\left(1 - \gamma_\circ^{-2}\right)\left[1 + (M_{cbm}/M_B) + (M_{cbm}/M_B)^2\right]}}{1 + (M_{cbm}/M_B)\left(1 + \gamma_\circ^{-1}\right)\left[1 + \frac{1}{2}(M_{cbm}/M_B)\right]}. \tag{E.1.3}$$

Using the analytic expression for the EQTS given in Bianco and Ruffini (2005b) and in Eq.(D.2.1), Eq.(E.1.2) takes the form (Bianco and Ruffini, 2006):

$$\begin{cases} \cos\vartheta_\circ = \dfrac{\sqrt{\left(1-\gamma_\circ^{-2}\right)\left[1+(M_{cbm}/M_B)+(M_{cbm}/M_B)^2\right]}}{1+(M_{cbm}/M_B)\left(1+\gamma_\circ^{-1}\right)\left[1+\frac{1}{2}\left(M_{cbm}/M_B\right)\right]} \\[2ex] \cos\vartheta_\circ = \dfrac{M_B-m_i^\circ}{2r\sqrt{C}}\left(r-r_\circ\right) + \dfrac{m_i^\circ r_\circ}{8r\sqrt{C}}\left[\left(\dfrac{r}{r_\circ}\right)^4 - 1\right] \\[2ex] \qquad\quad + \dfrac{r_\circ\sqrt{C}}{12rm_i^\circ A^2}\ln\left\{\dfrac{[A+(r/r_\circ)]^3\left(A^3+1\right)}{\left[A^3+(r/r_\circ)^3\right](A+1)^3}\right\} \\[2ex] \qquad\quad + \dfrac{ct_\circ}{r} - \dfrac{c(t_a^d)_{jet}}{r(1+z)} + \dfrac{r^\star}{r} \\[2ex] \qquad\quad + \dfrac{r_\circ\sqrt{3C}}{6rm_i^\circ A^2}\left[\arctan\dfrac{2(r/r_\circ)-A}{A\sqrt{3}} - \arctan\dfrac{2-A}{A\sqrt{3}}\right] \end{cases} \tag{E.1.4}$$

where $t_\circ$ is the value of the time t at the beginning of the afterglow phase, $m_i^\circ = (4/3)\pi m_p n_{cbm} r_\circ^3$, $r^\star$ is the initial size of the expanding source, $A = [(M_B - m_i^\circ)/m_i^\circ]^{1/3}$, $C = M_B^2(\gamma_\circ - 1)/(\gamma_\circ + 1)$ and z is the cosmological redshift of the source.

E.1.2. The adiabatic regime

In this case, the analytic solution of the equations of motion gives (see Eq.(C.2.2) and Bianco and Ruffini, 2005b,a):

$$\frac{v}{c} = \sqrt{\gamma_\circ^2 - 1}\left(\gamma_\circ + \frac{M_{cbm}}{M_B}\right)^{-1} \tag{E.1.5}$$

Using the analytic expression for the EQTS given in Bianco and Ruffini (2005b) and in Eq.(D.2.2), Eq.(E.1.2) takes the form (Bianco and Ruffini, 2006):

$$
\begin{cases}
\cos\vartheta_\circ = \sqrt{\gamma_\circ^2 - 1}\left(\gamma_\circ + \frac{M_{cbm}}{M_B}\right)^{-1} \\[2ex]
\cos\vartheta_\circ = \frac{m_i^\circ}{4M_B\sqrt{\gamma_\circ^2-1}}\left[\left(\frac{r}{r_\circ}\right)^3 - \frac{r_\circ}{r}\right] + \frac{ct_\circ}{r} \\[1ex]
\qquad - \frac{c(t_a^d)_{jet}}{r(1+z)} + \frac{r^\star}{r} - \frac{\gamma_\circ - \left(m_i^\circ/M_B\right)}{\sqrt{\gamma_\circ^2-1}}\left[\frac{r_\circ}{r} - 1\right]
\end{cases}
\qquad \text{(E.1.6)}
$$

where all the quantities have the same definition as in Eq.(E.1.4).

E.1.3. The comparison between the two solutions

In Fig. E.1 we plot the numerical solutions of both Eq.(E.1.4), corresponding to the fully radiative regime, and Eq.(E.1.6), corresponding to the adiabatic one. Both curves have been plotted assuming the same initial conditions, namely the ones of GRB 991216 (see Ruffini et al., 2003).

E.2. Comparison with the existing literature

Three different approximated formulas for the relation between $(t_a^d)_{jet}$ and $\vartheta_\circ$ have been given in the current literature, all assuming the adiabatic regime. Panaitescu and Mészáros (1999) proposed:

$$
\cos\vartheta_\circ \simeq 1 - 5.9 \times 10^7 \left(\frac{n_{cbm}}{E}\right)^{1/4}\left[\frac{(t_a^d)_{jet}}{1+z}\right]^{3/4}, \qquad \text{(E.2.1)}
$$

Sari et al. (1999), instead, advanced:

$$
\vartheta_\circ \simeq 7.4 \times 10^3 \left(\frac{n_{cbm}}{E}\right)^{1/8}\left[\frac{(t_a^d)_{jet}}{1+z}\right]^{3/8}. \qquad \text{(E.2.2)}
$$

In both Eq.(E.2.1) and Eq.(E.2.2), $(t_a^d)_{jet}$ is measured in seconds, E is the source initial energy measured in ergs and n_{cbm} is the CBM number density in particles/cm^3. The formula by Sari et al. (1999) has been applied quite often in the current literature (see e.g. Frail et al., 2001; Ghirlanda et al., 2004; Fox et al., 2005).

Both Eq.(E.2.1) and Eq.(E.2.2) compute the arrival time of the photons at the detector assuming that all the radiation is emitted at $\vartheta = 0$ (i.e. on the line of sight), neglecting the full shape of the EQTSs. Recently, a new expression
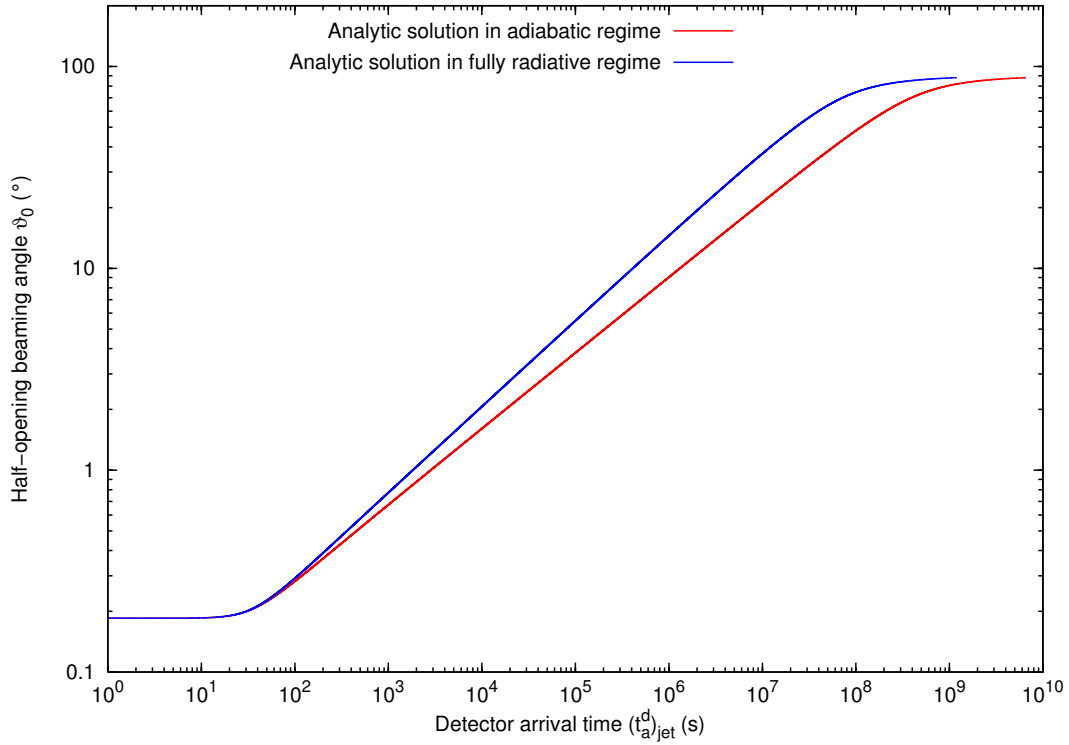
Figure E.1.: Comparison between the numerical solution of Eq.(E.1.4) assuming fully radiative regime (blue line) and the corresponding one of Eq.(E.1.6) assuming adiabatic regime (red line). The departure from power-law behavior at small arrival time follows from the constant Lorentz γ factor regime, while the one at large angles follows from the approach to the non-relativistic regime (see details in Fig. E.4, as well as in Bianco and Ruffini, 2005a, 2006).
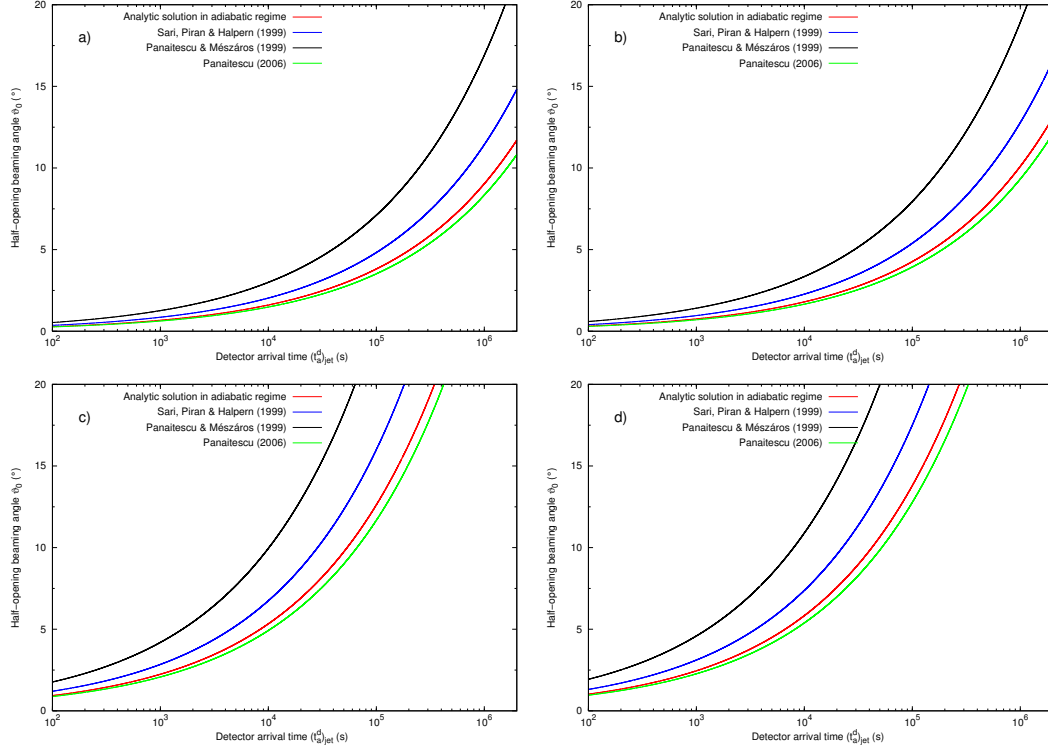
Figure E.2.: Comparison between the numerical solution of Eq.(E.1.6) (red line) and the corresponding approximate formulas given in Eq.(E.2.2) (blue line), in Eq.(E.2.1) (black line), and in Eq.(E.2.3) (green line). All four curves have been plotted for four different GRBs: a) GRB 991216 (Ruffini et al., 2003), b) GRB 980519 (Ruffini et al., in preparation), c) GRB 031203 (Bernardini et al., 2005), d) GRB 980425 (Ruffini et al., 2004a, 2007). The ranges of the two axes have been chosen to focus on the sole domains of application of the approximate treatments in the current literature. Details in Bianco and Ruffini (2006).

has been proposed by Panaitescu (2006), again neglecting the full shape of the EQTSs but assuming that all the radiation is emitted from $\vartheta = 1/\gamma$, i.e. from the boundary of the visible region. Such an expression is:

$$\vartheta_\circ \simeq 5.4 \times 10^3 \left(\frac{n_{cbm}}{E} \right)^{1/8} \left[\frac{(t_a^d)_{jet}}{1+z} \right]^{3/8} . \tag{E.2.3}$$

In Fig. E.2 we plot Eq.(E.2.1), Eq.(E.2.2) and Eq.(E.2.3) together with the numerical solution of Eq.(E.1.6) relative to the adiabatic regime. All four curves have been plotted assuming the same initial conditions for four different GRBs, encompassing more than 5 orders of magnitude in energy and more than 2 orders of magnitude in CBM density:

- GRB 991216 (Ruffini et al., 2003),

- GRB 980519 (Ruffini et al., in preparation),

- GRB 031203 (Bernardini et al., 2005),

- GRB 980425 (Ruffini et al., 2004a, 2007).

The approximate Eq.(E.2.2) by Sari et al. (1999) and Eq.(E.2.3) by Panaitescu (2006) both imply a power-law relation between $\vartheta_\circ$ and $(t_a^d)_{jet}$ with constant index 3/8 for any value of $\vartheta_\circ$, while Eq.(E.2.1) by Panaitescu and Mészáros (1999) implies a power-law relation with constant index 3/8 only for $\vartheta_\circ \to 0$ (for greater $\vartheta_\circ$ values the relation is trigonometric).

All the above three approximate treatments are based on the approximate power-law solutions of the GRB afterglow dynamics which have been shown in the previous sections and in Bianco and Ruffini (2005a) to be not applicable to GRBs. They also do not take fully into account the structure of the EQTSs, although in different ways. Both Eq.(E.2.1) and Eq.(E.2.2), which assume all the radiation coming from $\vartheta = 0$, overestimate the behavior of the exact solution. On the other hand, Eq.(E.2.3), which assumes all the radiation coming from $\vartheta \sim 1/\gamma$, is a better approximation than the previous two, but still slightly underestimates the exact solution.

E.3. An empirical fit of the numerical solution

For completeness, we now fit our exact solution with a suitable explicit functional form in the four cases considered in Fig. E.2. We chose the same functional form of Eq.(E.2.3), which is the closer one to the numerical solution,
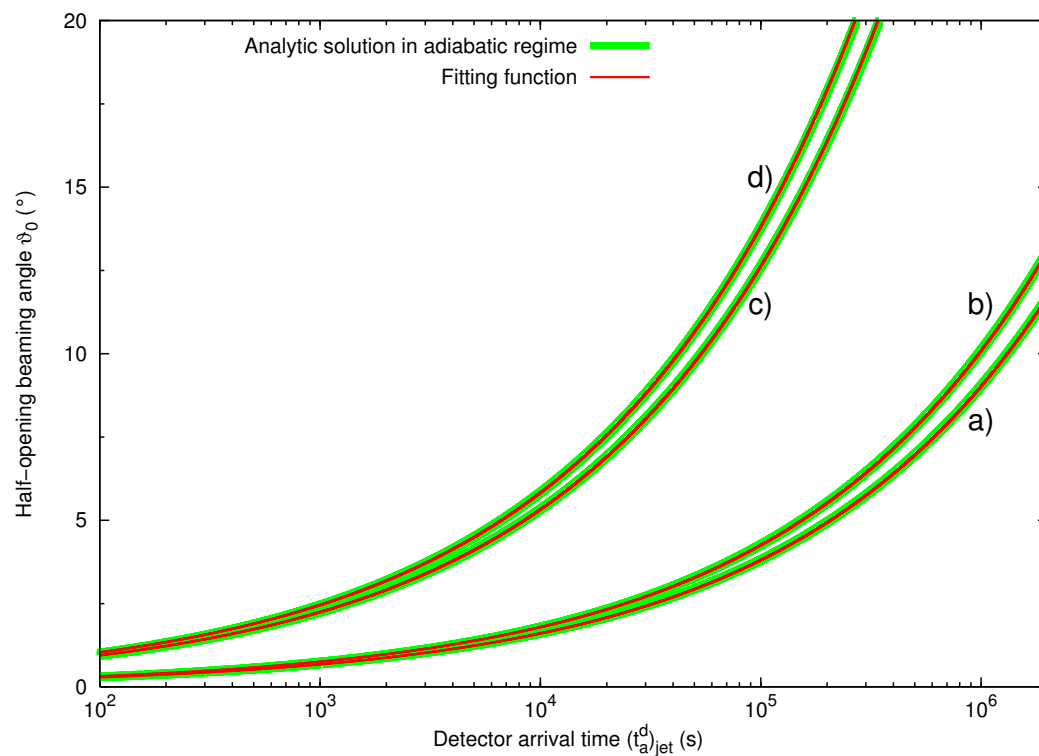
Figure E.3.: The overlapping between the numerical solution of Eq.(E.1.6) (thick green lines) and the approximate fitting function given in Eq.(E.3.1) (thin red lines) is shown in the four cases (a–d) represented in Fig. E.2.
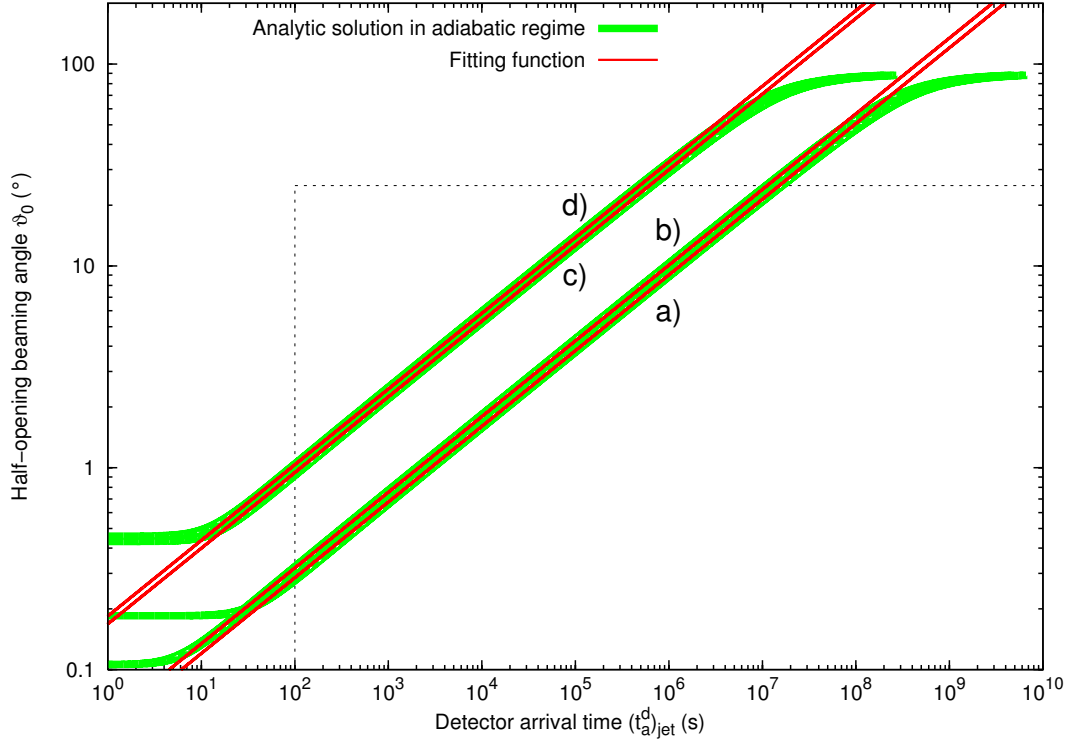
Figure E.4.: Comparison between the numerical solution of Eq.(E.1.6) (think green lines) and the approximate fitting function given in Eq.(E.3.1) (thin red lines) in all the four cases (a–d) represented in Fig. E.2. The ranges of the two axes have been chosen to have their full extension (i.e. the one of Fig. E.1). The dashed gray lines are the boundaries of the region where the empirical fitting function can be applied. Details in Bianco and Ruffini (2006).

using the numerical factor in front of it (i.e. 5.4×10^3) as the fitting parameter. We find that the following approximate expression (Bianco and Ruffini, 2006):

$$\vartheta_\circ \simeq 5.84 \times 10^3 \left(\frac{n_{cbm}}{E}\right)^{1/8} \left[\frac{(t_a^d)_{jet}}{1+z}\right]^{3/8} \tag{E.3.1}$$

is in agreement with the numerical solution in all the four cases presented in Fig. E.2 (see Fig. E.3). However, if we enlarge the axis ranges to their full extension (i.e. the one of Fig. E.1), we see that such approximate empirical fitting formula can only be applied for $\vartheta_\circ < 25°$ *and* $(t_a^d)_{jet} > 10^2$ s (see the gray dashed rectangle in Fig. E.4).

An equivalent empirical fit in the fully radiative regime is not possible. In this case, indeed, there is a domain in the $((t_a^d)_{jet}, \vartheta_\circ)$ plane where the numer-

ical solution shows a power-law dependence on time, with an index ~ 0.423 (see Fig. E.1). However, the dependence on the energy cannot be factorized out with a simple power-law. Therefore, in the fully radiative regime, which is the relevant one for our GRB model (see e.g. Ruffini et al., 2003), the application of the full Eq.(E.1.4) does not appear to be avoidable.

Bibliography

BERNARDINI, M.G., BIANCO, C.L., CHARDONNET, P., FRASCHETTI, F., RUFFINI, R. AND XUE, S.S.
《Theoretical interpretation of the luminosity and spectral properties of grb 031203》.
ApJ, **634**, pp. L29–L32 (2005).

BIANCO, C.L. AND RUFFINI, R.
《Exact versus approximate equitemporal surfaces in gamma-ray burst afterglows》.
ApJ, **605**, pp. L1–L4 (2004).

BIANCO, C.L. AND RUFFINI, R.
《Exact versus approximate solutions in gamma-ray burst afterglows》.
ApJ, **633**, pp. L13–L16 (2005a).

BIANCO, C.L. AND RUFFINI, R.
《On the exact analytic expressions for the equitemporal surfaces in gamma-ray burst afterglows》.
ApJ, **620**, pp. L23–L26 (2005b).

BIANCO, C.L. AND RUFFINI, R.
《Exact versus approximate beaming formulae in gamma-ray burst afterglows》.
ApJ, **644**, pp. L105–L108 (2006).

BIANCO, C.L., RUFFINI, R. AND XUE, S.S.
《The elementary spike produced by a pure e^+e^- pair-electromagnetic pulse from a black hole: The pem pulse》.
A&A, **368**, pp. 377–390 (2001).

BLANDFORD, R.D. AND MCKEE, C.F.
《Fluid dynamics of relativistic blast waves》.
Physics of Fluids, **19**, pp. 1130–1138 (1976).

CHIANG, J. AND DERMER, C.D.
《Synchrotron and synchrotron self-compton emission and the blast-wave model of gamma-ray bursts》.
ApJ, **512**, pp. 699–710 (1999).

COUDERC, P.
«Les auréoles lumineuses des novae».
Annales d'Astrophysique, **2**, p. 271 (1939).

FOX, D.B., FRAIL, D.A., PRICE, P.A., KULKARNI, S.R., BERGER, E., PIRAN, T., SODERBERG, A.M., CENKO, S.B., CAMERON, P.B., GAL-YAM, A. ET AL.
«The afterglow of grb 050709 and the nature of the short-hard γ-ray bursts».
Nature, **437**, pp. 845–850 (2005).

FRAIL, D.A., KULKARNI, S.R., NICASTRO, L., FEROCI, M. AND TAYLOR, G.B.
«The radio afterglow from the γ-ray burst of 8 May 1997».
Nature, **389**, pp. 261–263 (1997).

FRAIL, D.A., KULKARNI, S.R., SARI, R., DJORGOVSKI, S.G., BLOOM, J.S., GALAMA, T.J., REICHART, D.E., BERGER, E., HARRISON, F.A., PRICE, P.A. ET AL.
«Beaming in gamma-ray bursts: Evidence for a standard energy reservoir».
ApJ, **562**, pp. L55–L58 (2001).

GALAMA, T.J., FRAIL, D.A., SARI, R., BERGER, E., TAYLOR, G.B. AND KULKARNI, S.R.
«Continued Radio Monitoring of the Gamma-Ray Burst 991208».
ApJ, **585**, pp. 899–907 (2003).

GARNAVICH, P.M., LOEB, A. AND STANEK, K.Z.
«Resolving Gamma-Ray Burst 000301C with a Gravitational Microlens».
ApJ, **544**, pp. L11–L15 (2000).

GAUDI, B.S., GRANOT, J. AND LOEB, A.
«Microlensing and the Surface Brightness Profile of the Afterglow Image of Gamma-Ray Burst 000301C».
ApJ, **561**, pp. 178–182 (2001).

GHIRLANDA, G., GHISELLINI, G. AND LAZZATI, D.
«The collimation-corrected gamma-ray burst energies correlate with the peak energy of their νf_ν spectrum».
ApJ, **616**, pp. 331–338 (2004).

GRANOT, J.
«Analytic expressions for the surface brightness profile of gamma-ray burst afterglow images».

MNRAS, **390**, pp. L46–L50 (2008).

GRANOT, J. AND LOEB, A.
«Chromatic Signatures in the Microlensing of Gamma-Ray Burst After-glows».
ApJ, **551**, pp. L63–L66 (2001).

GRANOT, J. AND LOEB, A.
«Radio Imaging of Gamma-Ray Burst Jets in Nearby Supernovae».
ApJ, **593**, pp. L81–L84 (2003).

GRANOT, J., PIRAN, T. AND SARI, R.
«Images and spectra from the interior of a relativistic fireball».
ApJ, **513**, pp. 679–689 (1999a).

GRANOT, J., PIRAN, T. AND SARI, R.
«Synchrotron Self-Absorption in Gamma-Ray Burst Afterglow».
ApJ, **527**, pp. 236–246 (1999b).

GRANOT, J., RAMIREZ-RUIZ, E. AND LOEB, A.
«Implications of the Measured Image Size for the Radio Afterglow of GRB 030329».
ApJ, **618**, pp. 413–425 (2005).

GRUZINOV, A. AND WAXMAN, E.
«Gamma-ray burst afterglow: Polarization and analytic light curves».
ApJ, **511**, pp. 852–861 (1999).

HUANG, Y.F., CHENG, K.S. AND GAO, T.T.
«Modeling the Optical Afterglow of GRB 030329».
ApJ, **637**, pp. 873–879 (2006).

HUANG, Y.F., LU, Y., WONG, A.Y.L. AND CHENG, K.S.
«A Detailed Study on the Equal Arrival Time Surface Effect in Gamma-Ray Burst Afterglows».
Chinese Journal of Astronomy and Astrophysics, **7**, pp. 397–404 (2007).

IOKA, K. AND NAKAMURA, T.
«Microlensing of Collimated Gamma-Ray Burst Afterglows».
ApJ, **561**, pp. 703–707 (2001).

MAO, S. AND YI, I.
«Relativistic beaming and gamma-ray bursts».
ApJ, **424**, pp. L131–L134 (1994).

MÉSZÁROS, P.
    «Theories of gamma-ray bursts».
    ARAA, **40**, pp. 137–169 (2002).

MESZAROS, P.
    «Gamma-ray bursts.»
    Reports of Progress in Physics, **69**, pp. 2259–2322 (2006).

OREN, Y., NAKAR, E. AND PIRAN, T.
    «The apparent size of gamma-ray burst afterglows as a test of the fireball model».
    MNRAS, **353**, pp. L35–L40 (2004).

PANAITESCU, A.
    «The energetics and environment of the short-grb afterglows 050709 and 050724».
    MNRAS, **367**, pp. L42–L46 (2006).

PANAITESCU, A. AND MESZAROS, P.
    «Rings in fireball afterglows».
    ApJ, **493**, p. L31 (1998).

PANAITESCU, A. AND MÉSZÁROS, P.
    «Dynamical evolution, light curves, and spectra of spherical and collimated gamma-ray burst remnants».
    ApJ, **526**, pp. 707–715 (1999).

PIHLSTRÖM, Y.M., TAYLOR, G.B., GRANOT, J. AND DOELEMAN, S.
    «Stirring the Embers: High-Sensitivity VLBI Observations of GRB 030329».
    ApJ, **664**, pp. 411–415 (2007).

PIRAN, T.
    «Gamma-ray bursts and the fireball model».
    Phys. Rep., **314**, pp. 575–667 (1999).

PIRAN, T.
    «Gamma-ray bursts - a puzzle being resolved.»
    Phys. Rep., **333**, pp. 529–553 (2000).

PIRAN, T.
    «The physics of gamma-ray bursts».
    Reviews of Modern Physics, **76**, pp. 1143–1210 (2005).

REES, M.J.
    «Appearance of relativistically expanding radio sources».
    Nature, **211**, p. 468 (1966).

REES, M.J. AND MESZAROS, P.
≪Refreshed shocks and afterglow longevity in gamma-ray bursts≫.
ApJ, **496**, p. L1 (1998).

RUFFINI, R., AKSENOV, A.G., BERNARDINI, M.G., BIANCO, C.L., CAITO, L., CHARDONNET, P., DAINOTTI, M.G., DE BARROS, G., GUIDA, R., IZZO, L. ET AL.
≪The Blackholic energy and the canonical Gamma-Ray Burst IV: the "long," "genuine short" and "fake-disguised short" GRBs≫.
In M. Novello and S. Perez Bergliaffa (eds.), *XIII Brazilian School on Cosmology and Gravitation*, volume 1132 of *American Institute of Physics Conference Series*, pp. 199–266 (2009).

RUFFINI, R., BERNARDINI, M.G., BIANCO, C.L., CAITO, L., CHARDONNET, P., DAINOTTI, M.G., FRASCHETTI, F., GUIDA, R., VERESHCHAGIN, G. AND XUE, S.S.
≪The role of grb 031203 in clarifying the astrophysical grb scenario≫.
In S. Grebenev, R. Sunyaev, C. Winkler, A. Parmar and L. Ouwehand (eds.), *The 6th Integral Workshop - The Obscured Universe*, volume SP-622 of *ESA Special Publication*, p. 561 (2007).

RUFFINI, R., BERNARDINI, M.G., BIANCO, C.L., CHARDONNET, P., FRASCHETTI, F., GURZADYAN, V., VITAGLIANO, L. AND XUE, S.S.
≪The blackholic energy: long and short gamma-ray bursts (new perspectives in physics and astrophysics from the theoretical understanding of gamma-ray bursts, ii)≫.
In M. Novello and S.E. Perez Bergliaffa (eds.), *XI Brazilian School of Cosmology and Gravitation*, volume 782 of *American Institute of Physics Conference Series*, pp. 42–127 (2005).

RUFFINI, R., BERNARDINI, M.G., BIANCO, C.L., CHARDONNET, P., FRASCHETTI, F. AND XUE, S.S.
≪Grb 980425, sn1998bw and the embh model≫.
Advances in Space Research, **34**, pp. 2715–2722 (2004a).

RUFFINI, R., BERNARDINI, M.G., BIANCO, C.L., CHARDONNET, P., FRASCHETTI, F. AND XUE, S.S.
≪Evidence for isotropic emission in grb991216≫.
Advances in Space Research, **38**, pp. 1291–1294 (2006).

RUFFINI, R., BERNARDINI, M.G., BIANCO, C.L., CHARDONNET, P., FRASCHETTI, F. AND XUE, S.S. (in preparation).

RUFFINI, R., BIANCO, C.L., CHARDONNET, P., FRASCHETTI, F., GURZADYAN, V. AND XUE, S.S.
«On the instantaneous spectrum of gamma-ray bursts».
IJMPD, **13**, pp. 843–851 (2004b).

RUFFINI, R., BIANCO, C.L., CHARDONNET, P., FRASCHETTI, F., VITAGLIANO, L. AND XUE, S.S.
«New perspectives in physics and astrophysics from the theoretical understanding of gamma-ray bursts».
In M. Novello and S.E. Perez Bergliaffa (eds.), *Cosmology and Gravitation*, volume 668 of *American Institute of Physics Conference Series*, pp. 16–107 (2003).

RUFFINI, R., BIANCO, C.L., CHARDONNET, P., FRASCHETTI, F. AND XUE, S.S.
«On the interpretation of the burst structure of gamma-ray bursts».
ApJ, **555**, pp. L113–L116 (2001a).

RUFFINI, R., BIANCO, C.L., CHARDONNET, P., FRASCHETTI, F. AND XUE, S.S.
«Relative spacetime transformations in gamma-ray bursts».
ApJ, **555**, pp. L107–L111 (2001b).

RUFFINI, R., BIANCO, C.L., CHARDONNET, P., FRASCHETTI, F. AND XUE, S.S.
«On the structures in the afterglow peak emission of gamma-ray bursts».
ApJ, **581**, pp. L19–L22 (2002).

SAKAMOTO, T., BARBIER, L., BARTHELMY, S., CUMMINGS, J., FENIMORE, E., GEHRELS, N., HULLINGER, D., KRIMM, H., MARKWARDT, C., PALMER, D. ET AL.
«Grb 060218/sn 2006aj: Swift-bat fluence and peak flux.»
GCN Circ., **4822** (2006).

SARI, R.
«Hydrodynamics of gamma-ray burst afterglow».
ApJ, **489**, p. L37 (1997).

SARI, R.
«The observed size and shape of gamma-ray burst afterglow».
ApJ, **494**, p. L49 (1998).

SARI, R., PIRAN, T. AND HALPERN, J.P.
«Jets in gamma-ray bursts».
ApJ, **519**, pp. L17–L20 (1999).

TAYLOR, G.B., FRAIL, D.A., BERGER, E. AND KULKARNI, S.R.
≪The Angular Size and Proper Motion of the Afterglow of GRB 030329≫.
ApJ, **609**, pp. L1–L4 (2004).

TAYLOR, G.B., MOMJIAN, E., PIHLSTRÖM, Y., GHOSH, T. AND SALTER, C.
≪Late-Time Observations of the Afterglow and Environment of GRB 030329≫.
ApJ, **622**, pp. 986–990 (2005).

VAN PARADIJS, J., KOUVELIOTOU, C. AND WIJERS, R.A.M.J.
≪Gamma-ray burst afterglows≫.
ARAA, **38**, pp. 379–425 (2000).

WAXMAN, E.
≪Angular size and emission timescales of relativistic fireballs≫.
ApJ, **491**, p. L19 (1997).

WAXMAN, E., KULKARNI, S.R. AND FRAIL, D.A.
≪Implications of the Radio Afterglow from the Gamma-Ray Burst of 1997 May 8≫.
ApJ, **497**, p. 288 (1998).